TABLE 1. Concentrations (ng/L) of all-*trans*-4-oxo-RA, 13-*cis*-4-oxo-RA (n = 3), and the Chemical-Derived all-*trans*-RA Equivalents (ATRA-EQ_{cal}) in the Seven STP Influents and Effluents

	all-*trans*-4-oxo-RA		13-*cis*-4-oxo-RA		ATRA-EQ_{cal}	
	influent	effluent	influent	effluent	influent	effluent
Gaobeidian	5.9 ± 0.2	0.5 ± 0.1	2.7 ± 0.1	0.4 ± 0.1	23	2.0
Beixiaohe	4.7 ± 1.1	0.5 ± 0.0	2.5 ± 0.6	1.1 ± 0.4	18	2.3
Fangzhuang	10.4 ± 1.1	0.9 ± 0.1	7.1 ± 1.8	0.8 ± 0.2	41	3.7
Xiaohongmen	5.3 ± 0.2	nd[a]	3.1 ± 0.4	1.0 ± 0.4	21	0.8
Wujiacun	4.8 ± 0.6	nd	2.3 ± 0.1	nd	19	0.5
Jiuxianqiao	4.8 ± 0.7	nd	2.6 ± 0.1	0.7 ± 0.1	19	0.7
Qinghe	4.9 ± 0.7	nd	2.7 ± 0.0	nd	19	0.5

[a] nd = no detection.

activity profile of HPLC F15 in three subtypes (sensitivity decreased in the order of $\alpha > \gamma > \beta$) and its maximal activities are highly similar to those of all-*trans*-RA, suggesting that the RAR agonists in HPLC F15 might have a chemical structure similar to all-*trans*-RA. Therefore, the swine serum and human urine samples were also fractionated by HPLC, and significant RARα agonistic activities were also detected in the HPLC F15 of both samples. These results indicated that the RAR agonists in wastewater are endogenous RAs. To identify the potential chemical, three isomers of RA including all-*trans*-RA, 13-*cis*-RA, and 9-*cis*-RA were injected into the HPLC system. However, the peaks of the three isomers of RA did not overlap with HPLC F15 (Figure 3), indicating that these RAs were not the causative chemicals for the RAR agonistic activity in wastewater.

Thus, we tested two commercially obtainable metabolites of RAs, all-*trans*-4-oxo-RA and 13-*cis*-4-oxo-RA, which were reported to exhibit relatively high RAR-ligand affinity (*26, 27*). In our yeast assay for RARα-mediated activity, the EC_{50} for all-*trans*-4-oxo-RA was determined to be 0.32 nmol/L, much lower than all-*trans*-RA (1.35 nmol/L), while the EC_{50} for 13-*cis*-4-oxo-RA (3.2 nmol/L) was higher than that of all-*trans*-RA, as shown in Figure S5. The EC_{50} for all-*trans*-4-oxo-RA or 13-*cis*-4-oxo-RA relative to that of all-*trans*-RA was defined as its all-*trans*-RA equivalency factor (RAEF), which was calculated to be 3.87 and 0.46, respectively. As shown in Figure 3, the peaks of two isomers of 4-oxo-RA were observed at the retention times of 28.9 min (13-*cis*-4-oxo-RA) and 29.5 min (all-*trans*-4-oxo-RA), which overlapped with HPLC F15, suggesting that the 4-oxo-RAs might be the agonists of RAR in the samples. To further identify the causal chemicals inducing the RARα agonistic activity, UPLC fractionation for HPLC F15 from Gaobeidian STP influent was carried out, and the RARα activities of the fractions were also determined. As shown in Figure 4, the two bioactive fractions were found at the retention times of 3.5–4.0 min and 4.0–4.5 min (Figure 4A), overlapping with all-*trans*-4-oxo-RA and 13-*cis*-4-oxo-RA standards at 3.55 and 4.13 min, respectively (Figure 4B). In the influent sample (Figure 4C), two peaks were also found at 3.55 and 4.13 min by detecting a 315 m/z to 241 m/z MRM transition, which were highly suspected to be all-*trans*-4-oxo-RA and 13-*cis*-4-oxo-RA. Figure S6 shows the MS/MS spectra of the base peak ion of m/z 315 (ESI positive ion mode) in two bioactive fractions, and we found that the mass spectra at 3.55 and 4.13 min are highly similar to those of all-*trans*-4-oxo-RA and 13-*cis*-4-oxo-RA standards (Figure S2), suggesting that all-*trans*-4-oxo-RA and 13-*cis*-4-oxo-RA contributed to the RAR agonistic activity in the STP.

The HPLC F15 samples in the seven STPs, of which the RARα agonistic activities were reported above, were also analyzed by UPLC-ESI-MS/MS, and the concentrations in the influent and effluent samples without recovery correction are listed in Table 1. The concentrations of all-*trans*-4-oxo-RA were in the range of 4.7 to 10.4 ng/L in influents and below detection limit (<0.2 ng/L) to 0.9 ng/L in effluents, while the concentrations of 13-*cis*-4-oxo-RA were in the range of 2.3 to 7.1 ng/L in influents and below detection limit (<0.4 ng/L) to 1.1 ng/L in effluents. Based on the concentrations of all-*trans*-4-oxo-RA and 13-*cis*-4-oxo-RA and their RAEF values, the chemical-derived all-*trans*-RA equivalents (ATRA-EQ_{cal}) were calculated to be in the ranges of 18 ng/L (Beixiaohe STP) to 41 ng/L (Fangzhuang STP) and 0.5 ng/L (Wujiacun STP) to 3.7 ng/L (Fangzhuang STP) in influent and effluent, respectively.

For the river water samples, the concentrations of all-*trans*-4-oxo-RA were in the range of below detection limit (<0.2 ng/L) to 1.0 ng/L in summer and <0.2 to 1.8 ng/L in winter, while the concentrations of 13-*cis*-4-oxo-RA were in the ranges of below detection limit (<0.4 ng/L) to 1.6 ng/L in summer and <0.4 to 1.5 ng/L in winter (Tables S5 and S6). It should be noted that the ATRA-EQ_{cal} of samples taken at 4 and 2 km upstream Qing River in summer were much lower than the corresponding ATRA-EQ values derived from bioassay (Table S4), suggesting that there would be other unidentified RAR agonists in the river water and need to be studied further.

Previous studies have reported that all-*trans*-4-oxo-RA and 13-*cis*-4-oxo-RA widely exist in human and animal serum (*36, 37*) and can be eliminated from the body through urinary excretion (*38*). In another study, Li et al. also detected the glucuronide conjugate of all-*trans*-4-oxo-RA and 13-*cis*-4-oxo-RA in urine of rats that had been fed with all-*trans*-RA, 9-*cis*-RA, and 13-*cis*-RA previously (*39*). Thus, it is possible that all-*trans*-4-oxo-RA and 13-*cis*-4-oxo-RA can be produced through deconjugation of their glucuronides in wastewater treatment plants or rivers. In this study, however, we did not aim at the fates of all-*trans*-4-oxo-RA and 13-*cis*-4-oxo-RA in STP and their receiving river waters, and there is a need for further study.

All-*trans*-4-oxo-RA has been found to be much more active than all-*trans*-RA in causing microcephaly in *Xenopus laevis* embryos (*27*). In this study, the causal chemicals inducing RAR activity in the environment were identified for the first time, and there is a need to further investigate their occurrence, fates, and ecotoxicity to assess their ecological risk.

Acknowledgments

Financial support from the National Natural Science Foundation of China [20777002, 40632009], National Basic Research Program of China [2007CB407304], and Japan New Energy and Industrial Technology Development Organization is gratefully acknowledged.

Supporting Information Available

Additional tables and figures. This material is available free of charge via the Internet at http://pubs.acs.org.

Literature Cited

(1) Purdom, C. E.; Hardiman, P. A.; Bye, V. J.; Eno, N. C.; Tyler, C. R.; Sumpter, J. P. Estrogenic effects of effluents from sewage treatment works. *Chem. Ecol.* **1994**, *8*, 275–285.

(2) Jobling, S.; Nolan, M.; Tyler, C. R.; Brighty, G.; Sumpter, J. P. Widespread sexual disruption in wild fish. *Environ. Sci. Technol.* **1998**, *32*, 2498–2506.

(3) Bell, B.; Spotila, J. R.; Congdon, J. High incidence of deformity in aquatic turtles in the John Heinz National Wildlife refuge. *Environ. Pollut.* **2006**, *142*, 457–465.

(4) Kingsford, M. J.; Suthers, I. M.; Gray, C. A. Exposure to sewage plumes and the incidence of deformities in larval fishes. *Mar. Pollut. Bull.* **1996**, *33*, 201–212.

(5) Desbrow, C.; Routledge, E. J.; Brighty, G. C.; Sumpter, J. P.; Waldock, M. Identification of estrogenic chemicals in STW effluent. 1. Chemical fractionation and in vitro biological screening. *Environ. Sci. Technol.* **1998**, *32*, 1549–1558.

(6) Snyder, S. A.; Villeneuve, D. L.; Snyder, E. M.; Giesy, J. P. Identification and quantification of estrogen receptor agonists in wastewater effluents. *Environ. Sci. Technol.* **2001**, *35*, 3620–3625.

(7) Rudel, R. A.; Melly, S. J.; Geno, P. W.; Sun, G.; Brody, J. G. Identification of alkylphenols and other estrogenic phenolic compounds in wastewater, septage, and groundwater on Cape Cod, Massachusetts. *Environ. Sci. Technol.* **1998**, *32*, 861–869.

(8) Chawla, A.; Repa, J. J.; Evans, R. M.; Mangelsdorf, D. J. Nuclear Receptors and Lipid Physiology: Opening the X-Files. *Science* **2001**, *294*, 1866.

(9) Vos, J. G.; Dybing, E.; Greim, H. A.; Ladefoged, O.; Lambré, C.; Tarazona, J. V.; Brandt, I.; Vethaak, A. D. Health effects of endocrine-disrupting chemicals on wildlife, with special reference to the European situation. *Crit. Rev. Toxicol.* **2000**, *30*, 71–133.

(10) Nishikawa, J.; Mamiya, S.; Kanayama, T.; Nishikawa, T.; Shiraishi, F.; Horiguchi, T. Involvement of the retinoid X receptor in the development of imposex caused by organotins in gastropods. *Environ. Sci. Technol.* **2004**, *38*, 6271–6276.

(11) Gudas, L. J.; Sporn, M. B.; Roberts, A. B. In *The Retinoids: Biology, Chemistry, and Medicine*; Sporn, M. B., Roberts, A. B., Goodman, D. S., Eds.; Raven Press: New York, 1994; pp 443–520.

(12) Collins, M. D.; Mao, G. E. Teratology of retinoids. *Annu. Rev. Pharmacol. Toxicol.* **1999**, *39*, 399–430.

(13) Chambon, P. A decade of molecular biology of retinoic acid receptors. *FASEB J.* **1996**, *10*, 940–954.

(14) Haga, Y.; Suzuki, T.; Takeuchi, T. Retinoic Acid isomers produce malformations in postembryonic development of the Japanese flounder *Paralichthys olivaceus*. *Zool. Sci.* **2002**, *19*, 1105–1112.

(15) Scadding, S. R.; Maden, M. Comparison of the effects of vitamin A on limb development and regeneration in *Xenopus laevis* tadpoles. *J. Embryol. Exp. Morphol.* **1986**, *91*, 35–53.

(16) Scadding, S. R.; Maden, M. The effects of local application of retinoic acid on limb development and regeneration in tadpoles of *Xenopus laevis*. *J. Embryol. Exp. Morphol.* **1986**, *91*, 55–63.

(17) Degitz, S. J.; Kosian, P. A.; Makynen, E. A.; Jensen, K. M.; Ankley, G. T. Stage- and Species-Specific Developmental Toxicity of All-Trans Retinoic Acid in Four Native North American *Ranids* and *Xenopus laevis*. *Toxicol. Sci.* **2000**, *57*, 264–74.

(18) Alsop, D. H.; Brown, S. B.; van der Kraak, G. J. Dietary retinoic acid induces hindlimb and eye deformities in *Xenopus laevis*. *Environ. Sci. Technol.* **2004**, *38*, 6290–6299.

(19) Gardiner, D. M.; Hoppe, D. M. Environmentally induced limb malformation in mink frogs (*Rana septentrionalis*). *J. Exp. Zool.* **1999**, *284*, 207–216.

(20) Meteyer, C. U.; Loeffler, I. K.; Fallon, J. F.; Converse, K. A. Hind limb malformations in free-living northern leopard frogs (*Rana pipiens*) from Maine, Minnesota, and Vermont suggest multiple etiologies. *Teratology* **2000**, *62*, 151–171.

(21) Ouellet, M.; Bonin, J.; Rodrigue, J.; DesGranges, J. L.; Lair, S. Hindlimb deformities (ectromelia, ectrodactyly) in free-living anurans from agricultural habitats. *J. Wildlife Dis.* **1997**, *33*, 95–104.

(22) Taylor, B.; Skelly, D.; Demarchis, L. K.; Slade, M. D.; Galusha, D.; Rabinowitz, P. M. Proximity to pollution sources and risk of amphibian limb malformation. *Environ. Health Perspect.* **2005**, *113*, 1497–1501.

(23) Gardiner, D.; Ndayibagira, A.; Grun, F.; Blumberg, B. Deformed frogs and environmental retinoids. *Pure Appl. Chem.* **2003**, *75*, 2263–2273.

(24) Peck, G. L.; DiGiovanna, J. J. In *The Retinoids: Biology, Chemistry, and Medicine*; Sporn, M. B.; Roberts, A. B., Goodman, D. S., Eds.; Raven Press: New York, 1994; pp 631–658.

(25) Hong, W. K.; Itri, L. M. In *The Retinoids: Biology, Chemistry, and Medicine*; Sporn, M. B., Roberts, A. B., Goodman, D. S., Eds.; Raven Press: New York, 1994; pp 597–630.

(26) Idres, N.; Marill, J.; Flexor, M. A.; Chabot, G. G. Activation of retinoic acid receptor-dependent transcription by all-trans-retinoic acid metabolites and isomers. *J. Biol. Chem.* **2002**, *277*, 31491–31498.

(27) Pijnappel, W. W. M.; Hendriks, H. F. J.; Folkers, G. E.; van den Brink, C. E.; Dekker, E. J.; Edelenbosch, C.; van der Saag, P. T.; Durston, A. J. The retinoid ligand 4-oxo-retinoic acid is a highly active modulator of positional specification. *Nature* **1993**, *366*, 340–344.

(28) Lemaire, G.; Balaguer, P.; Michel, S.; Rahmani, R. Activation of retinoic acid receptor-dependent transcription by organochlorine pesticides. *Toxicol. Appl. Pharmacol.* **2005**, *202*, 38–49.

(29) Kanayama, T.; Kobayashi, N.; Mamiya, S.; Nakanishi, T.; Nishikawa, J. Organotin compounds promote adipocyte differentiation as agonists of the Peroxisome Proliferator-Activated Receptor γ/Retinoid X Receptor Pathway. *Mol. Pharmacol.* **2005**, *67*, 766–774.

(30) Kamata, R.; Shiraishi, F.; Nishikawa, J.; Yonemoto, J.; Shiraishi, H. Screening and detection of the in vitro agonistic activity of xenobiotics on the retinoic acid receptor. *Toxicol. Vitro* **2008**, *22*, 1050–61.

(31) Alsop, D.; Hewitt, M.; Kohli, M.; Brown, S.; van der Kraak, G. Constituents within pulp mill effluent deplete retinoid stores in white sucker and bind to rainbow trout retinoic acid receptors and retinoid X receptors. *Environ. Toxicol. Chem./SETAC* **2003**, *22*, 2969–2976.

(32) Schmidt, C. K.; Volland, J.; Hamscher, G.; Nau, H. Characterization of a new endogenous vitamin A metabolite. *Biochim. Biophys. Acta Mol. Cell Biol. Lipids* **2002**, *1583*, 237–251.

(33) Nishikawa, J.; Saito, K.; Goto, J.; Dakeyama, F.; Matsuo, M.; Nishihara, T. New screening methods for chemicals with hormonal activities using interaction of nuclear hormone receptor with coactivator. *Toxicol. Appl. Pharmacol.* **1999**, *154*, 76–83.

(34) Villeneuve, D. L.; Blankenship, A. L.; Giesy, J. P. Derivation and application of relative potency estimates based on in vitro bioassay results. *Environ. Toxicol. Chem./SETAC* **2000**, *19*, 2835–2843.

(35) Chang, H.; Hu, J. Y.; Shao, B. Occurrence of natural and synthetic glucocorticoids in sewage treatment plants and receiving river waters. *Environ. Sci. Technol.* **2007**, *41*, 3462–3468.

(36) Gundersen, T. E.; Blomhoff, R. Qualitative and quantitative liquid chromatographic determination of natural retinoids in biological samples. *J. Chromatogr. A* **2001**, *935*, 13–43.

(37) Wyss, R.; Bucheli, F. Determination of endogenous levels of 13-*cis*-retinoic acid (isotretinoin), all-*trans*-retinoic acid (tretinoin) and their 4-oxo metabolites in human and animal plasma by high-performance liquid chromatography with automated column switching and ultraviolet detection. *J. Chromatogr. B* **1997**, *700*, 31–47.

(38) Marill, J.; Idres, N.; Capron, C. C.; Nguyen, E.; Chabot, G. G. Retinoic acid metabolism and mechanism of action: a review. *Curr. Drug Metab.* **2003**, *4*, 1–10.

(39) Li, S.; Barua, A. B.; Huselton, C. A. Quantification of retinoyl-β-glucuronides in rat urine by reversed phase high-performance liquid chromatography with ultraviolet detection. *J. Chromatogr. B* **1996**, *683*, 155–162.

ES9000328

The Journal of Toxicological Sciences (J. Toxicol. Sci.)
Vol.34, Special Issue II, SP279-SP286, 2009

Intrauterine environment-genome interaction and Children's development (2): Brain structure impairment and behavioral disturbance induced in male mice offspring by a single intraperitoneal administration of domoic acid (DA) to their dams

Kentaro Tanemura, Katsuhide Igarashi, Toshiko-R Matsugami, Ken-ichi Aisaki, Satoshi Kitajima and Jun Kanno

Division of Cellular & Molecular Toxicology, Biological Safety Research Center, National Institute of Health Sciences, 1-18-1 Kamiyoga, Setagaya-ku, Tokyo 158-8501, Japan

(Received February 17, 2009)

ABSTRACT — To demonstrate induction of delayed central nervous toxicity by disturbing neuronal activities in the developing brain, we administered a single intraperitoneal dose of domoic acid (DA; 1 mg/kg), a potent glutamate receptor agonist, to pregnant female mice at the gestational day of 11.5, 14.5 or 17.5. The dams had recovered from acute symptoms within 24 hr, followed by normal delivery, feeding and weaning. All male offspring mice after weaning were apparently normal in response to handlers during cage maintenance, body weight measurement and to mate mice in group housing conditions. At the age of 11 weeks, our neurobehavior testing battery revealed severe impairment of learning and memory with serious deviances of anxiety-related behaviors. The developed brain of prenatally exposed mice showed myelination failure and the overgrowth of neuronal processes of the limbic cortex neurons. This study indicates that the temporal disturbance of neurotransmission of the developing brain induces irreversible structural and functional damage to offspring which becomes monitorable in their adulthood by a proper battery of neurobehavioral tests.

Key words: Domoic acid, Prenatal exposure, Brain structure, Behavior

INTRODUCTION

Adequate neural activities are necessary for the maturation of neural networks during brain development (Rice and Barone, 2000). Historically, the presence of such plasticity-driven mechanisms has been demonstrated by a series of studies of eyelid suture in kittens or monkeys and corresponding findings reported in young human cataracta patients (Wiesel, 1982; Gu *et al.*, 1989; Fonta *et al.*, 2000). These processes require proper stimuli to the brain that trigger the release of neurotransmitters from the neurons and subsequent receptor-mediated signal transduction (Ooi and Wood, 2008; Greer and Greenberg, 2008; Cohen-Cory, 2002). Therefore, it is highly conceivable that disturbance of neural activities by neuroactive xenobiotics leads to malformation of the fine structure of the brain. Even when the exposure was transient, it would result in anomaly of higher brain functions in adulthood without overt signs of brain damage during maturation.

Glutamate receptors begin to express in the late embryonic stages, and their expression increases with the advance of brain development (Luján *et al.*, 2005; Manent *et al.*, 2005). Prenatal exposure of xenobiotic chemicals that interfere with the glutamate receptor function could induce malformation of the fine structure of the brain which should lead to anomaly of higher brain function that is different from acute neurotoxicity known for such chemicals to induce in adults (Bondy and Campbell, 2005). A marine biotoxin domoic acid (DA) which is structurally related to glutamate, and activates ionotropic α-amino-3-hydroxy-5-methyl-4-isoxazolepropionic acid (AMPA) and kinate subtypes of glutamate receptors (Pulido, 2008) is known to cause acute symptoms of diarrhea, seizures and memory loss in adult human by eating contaminated shellfish (Tryphonas and Iverson, 1990), and DA induced acute neurotoxicity in animal

Correspondence: Jun Kanno (E-mail: kanno@nihs.go.jp)

model (Chandrasekaran *et al.*, 2004). Additionally, DA is also known to cross the placenta, and enters prenatal brain tissue in rats (Maucher and Ramsdell, 2007). Therefore, prenatal exposure of DA may disrupt the neural activities by excessive stimulation of glutamate receptors, and should induce fine structural and functional disorganization in the developing brain. Here, we report that a transient transplacental DA exposure *in utero* induced alteration of the neurobehavioral parameters and corresponding fine brain structure of the male C57BL/6 mice in their adulthood.

MATERIALS AND METHODS

Animal treatment

All experiments were carried out under approval of Experimental Animal Use Committee of National Institute of Health Sciences, Japan. Pregnant C57LB/6 female mice obtained from Japan SLC, Inc., were individually housed in plastic breeding cages with free access to water and pellet diet (CRF-1; Oriental Yeast Co., Tokyo, Japan) in a 12 hr light-dark cycle conventional condition. Four groups with five pregnant mice each were prepared. All groups received three intraperitoneal injections on gestational day 11.5 (E11.5) as a late embryonic period, 14.5 (E14.5) and 17.5 (E17.5) as early and late fetal period respectively. Group A (Control) received three i.p. shots of saline on E11.5, E14.5 and E17.5. Group B (DA@ E11.5) received one shot of DA (Calbiochem, San Diego, CA, USA) at a dosage of 1 mg/kg on E 11.5 and two shots of saline on E14.5 and E17.5. Group C (DA@14.5) received a shot of saline on E11.5, a shot of DA on E14.5 and another saline on E17.5. Group D (DA@E17.5) received two shots of saline on E11.5 and E14.5 , and a shot of DA on E17.5. The pups were weaned at 4 weeks of age, and four male mice per liter were randomly selected and housed in one cage with free access to water and CRF-1 pellet until 11 weeks of age.

Immunohistochemical analysis

Brains (n = 4 male mice per group) were fixed with methacarn fixative (methanol: chloroform:acetic acid, 60:30:10 v/v) and paraffin-embedded sections were prepared. Mouse monoclonal anti-microtubule associated protein 2 (MAP2, sc-32791; Santa Cruz, CA, USA), mouse monoclonal anti-neurofilament-m (NF-M, sc-20013; Santa Cruz, CA, USA), rabbit polyclonal anti-myelin associated glycoprotein (MAG, sc-15324; Santa Cruz, CA, USA), and rabbit polyclonal anti MAP2 (sc-20172; Santa Cruz, CA, USA) were used. Deparaffinized sections were pretreated with HistoVT-One (Nacalai Tesque, Kyoto, Japan.) as previously described (Tanemura *et al.*, 2005) and incubated with primary antibodies. Secondary antibodies were Alexa 568-conjugated anti-mouse IgG and Alexa 488-conjugated anti-rabbit IgG (Molecular Probes, Eugene, OR, USA). Fluorescent images were obtained with an FV-300 confocal laser scanning microscope (Olympus, Tokyo, Japan). For semi-quantitative analysis of images, we calculated the ratio of fluorescence intensity compared to control mice (group A), by using the IMAGE J program (http://rsb.info.nih.gov/ij/index.html. National Institute of Health, Bethesda), after adjusting background noise (n = 4 images per mouse).

Neurobehavioral tests

A battery of neurobehavioral tests were conducted on open field test (OF), light/dark transition test (LD), elevated plus maze test (EP) and contextual/cued fear conditioning test (FZ). Experimental apparatuses and image analyzing softwares were obtained from O'Hara & Co., Ltd., Japan. Image analyzing softwares (Image OF4, Image LD2, Image EP2 and Image FZ2) were developed from the public domain IMAGE J program. All experiments were done with 8 mice per group (32 mice total), and were conducted between 13:30 and 16:30. The level of background noise during behavioural testing was about 50 dBA. After each trial, the apparatuses were wiped and cleaned.

Open field test

The locomotor activity was measured for 10 min using an open field apparatus made of white plastic (50 x 50 x 40 (H) cm).

An LED light system was positioned 50 cm above the centre of the field (50 lux at the centre of field). Total distance travelled (cm), time spent in the central area (30% of the field) (sec), and the frequencies of movement were measured (Tanemura *et al.*, 2002).

Light/dark transition test

The apparatus used for the light/dark transition test consisted of a cage (21 x 42 x 25(H) cm) divided into two chambers by a partition with an opening. One chamber is brightly illuminated (250 lux), whereas the other chamber is dark (2 lux). A mouse is placed into the dark area and allowed to move freely between the two chambers through the opening for 5 min. The latency for the first move to the light area, the total number of transitions and the time spent on each side were measured.

Elevated plus maze test

The plus-shaped apparatus consisted of four arms (25

x 5 cm) connected to a central square area (5 x 5 cm). Opposite two arms are enclosed with 20 cm-high transparent walls and other two are left open. The floor of the maze is made of white plastic plate and is elevated 60 cm above the room floor (200 lux at the centre of the apparatus). A mouse is placed to the central square area of the maze, facing one of the open arms, and the behavior was recorded for 10 min: total distance traveled (cm), total time on open arms and central square area (sec) and the total number of entry to any of the arms (Tanemura *et al.*, 2002).

Contextual/cued fear conditioning test

The apparatus consists of a conditioning chamber (or a test chamber) (17 x 10 x 10 (H) cm) made of clear plastic with ceiling and placed in a sound proof box. The chamber floor has stainless steel rods (2-mm diameter) spaced 5 mm apart for giving electric foot shock (0.1 mA, 3 sec duration) to the mouse. The soundproof box consists of white-coloured wood, and is equipped with an audio speaker and light source (35 lux at the centre of the floor). A CCD camera is positioned 20 cm above the ceiling of the chamber. During the conditioning trial (Day 1), mice are placed individually into the conditioning chamber in the sound proof box and, after 90 sec, they are given three tone-shock pairings (30 sec of tone, 75 dB, 10 KHz followed by 3 sec of electric shock at the end of tone, 0.1 mA) separated by 90 sec. Then they are returned to their home cage. Next day (Day 2), as a "contextual fear test", they are returned to the conditioning chamber without tone and shock for a 6-min. On the third day (Day 3), they are brought to a novel chamber of different make without stainless steel rods place in the sound proof box and, after a period of 3 min, only the conditioning tone is presented for 3 min (no shock was presented, 35 lux at the centre of the floor). The freezing response of mice was defined as a consecutive 2 sec period of immobility. Freezing rate (%) was calculated as [time freezing/session time] x 100 (Tatebayashi *et al.*, 2002).

Statistical analysis

Data were indicated as means ± S.D. Statistical analysis was conducted with student's t-test by using StatView (SAS Institute, Cary, NC, USA). A p-value of < 0.05 compared to the results of control male mice (group A) was considered statistically significant.

RESULTS

Effects on morphology of brain by prenatal exposure to DA

Offspring mice of all groups after weaning up to the age of 11 weeks were apparently normal in response to handlers during cage maintenance, body weight measurement and to mate mice in group housing conditions. Routine histological observation of the brain at 11 weeks old by hematoxylin-eosin staining could not reveal difference among the groups (data not shown). By immunohistochemical study on the same brain sections, reduced immuno-reactivity against the MAG, the marker for myelin, was detected in the cortices of group B (DA@11.5) and C (DA@14.5) compared to control (Figs. 1A-D and I). In contrast, increased immuno-reactivity against MAP2, the marker for neuronal dendrite, was indicated in the same area of group B (DA@11.5), C (DA@14.5) and D (DA@17.5) compared to control (Figs. 1E-H and J). Increased immuno-reactivity against MAP2 was also found in lateral area of CA3 hippocampus of group B (DA@11.5), C (DA@14.5) and D (DA@17.5) compared to control, whereas immuno-reactivity for MAP2 showed no significant difference in medial area of CA3 hippocampus among the groups (Figs. 2A-D and I). Immuno-reactivity against NF-M; the marker for neuronal axon, also showed no significant difference in the same area among the groups (Figs. 2E-H and J).

Effects on behavior by prenatal exposure of DA

In the OF test, the distance traveled was not different among the groups (Fig. 3A), the time spent in center area was significantly prolonged in group D (DA@17.5) mice (Fig. 3B). In the LD test, group C (DA@14.5) mice stayed in light area for longer time (Fig. 4A), and latency for the first move to light area was significantly shorter in group C (DA@14.5) and D (DA@17.5) (Fig. 4B). In the EP test, significantly increased distance traveled and time spent in the open area were detected for group B (DA@11.5), C (DA@14.5) and D (DA@17.5) (Figs. 5A and B). In the FZ test, both Day 1 and Day 2 freezing responses of group C (DA@14.5) and D (DA@17.5) were significantly reduced compared to control (Figs. 6A and B).

DISCUSSION

The expression levels of glutamate receptors starts to elevate at the fetal period, i.e. approximately from E14 (Luján *et al.*, 2005; Manent *et al.*, 2005). Exogenous glutamatergic stimuli at this period would affect the for-

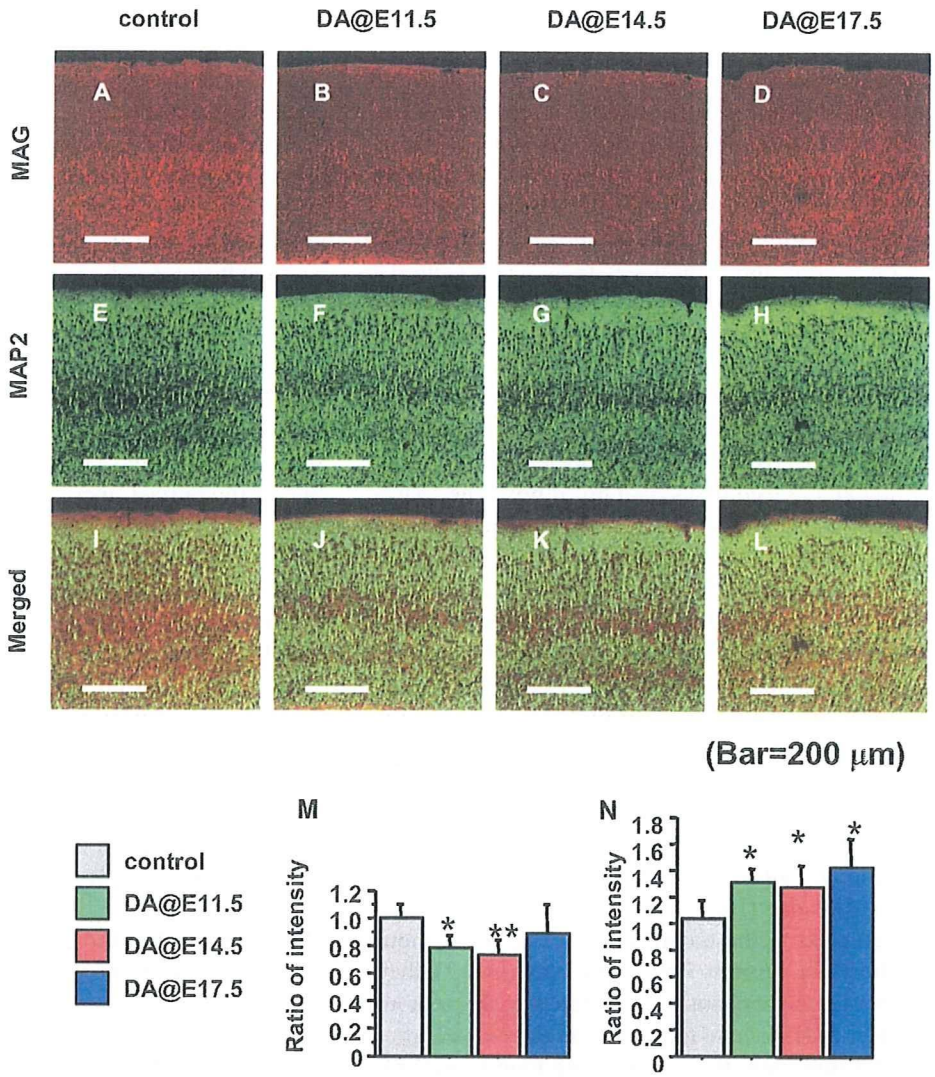

Fig. 1. Delayed effects on cerebral cortex induced by prenatal exposure of DA.
A-D, Immunohistochemical staining against MAG; E-H, immunohistochamical staining against MAP2; I-L, merged images of the cerebral cortex. A, E, I, group A (control), B, F, J, group B (DA@11.5), C, G, K, group C (DA@14.5) and D, H, L, group D (DA@17.5). Scale bar = 200 mm. M, Quantitative analysis in intensity ratio to control of MAG expression, and J, MAP2 expression among the groups (mean ± S.E.M.). Asterisk (**) and (*) indicate significant difference compared to control ($P < 0.01$) and ($P < 0.05$).

mation of the neural circuits. An extreme example to support this hypothesis would be the phenotype of the double knockout mouse of glutamate transportors GLT1 and GLAST (Matsugami *et al.*, 2006). Lack of these transportors is considered to result in abnormally high concentration of glutamate in the brain. In fact, morphological anomaly became apparent in synchronization with the expression of glutamine receptors. In our study, corresponding to the hypothesis, the neurobehavioral symptoms as a whole was severer for those exposed at fetal periods, i.e. E14.5 and E17.5, compared to those at embryonic period, i.e. E11.5 (Fig. 7).

We demonstrated that a prenatal exposure of a relatively low dose of DA induced a spectrum of neurobehavioral anomalies which became monitorable at the adult stage accompanied by alteration in fine brain structures detectable by immunohistochemistry. It is emphasized that this amount of DA did not induce abnormal responses dur-

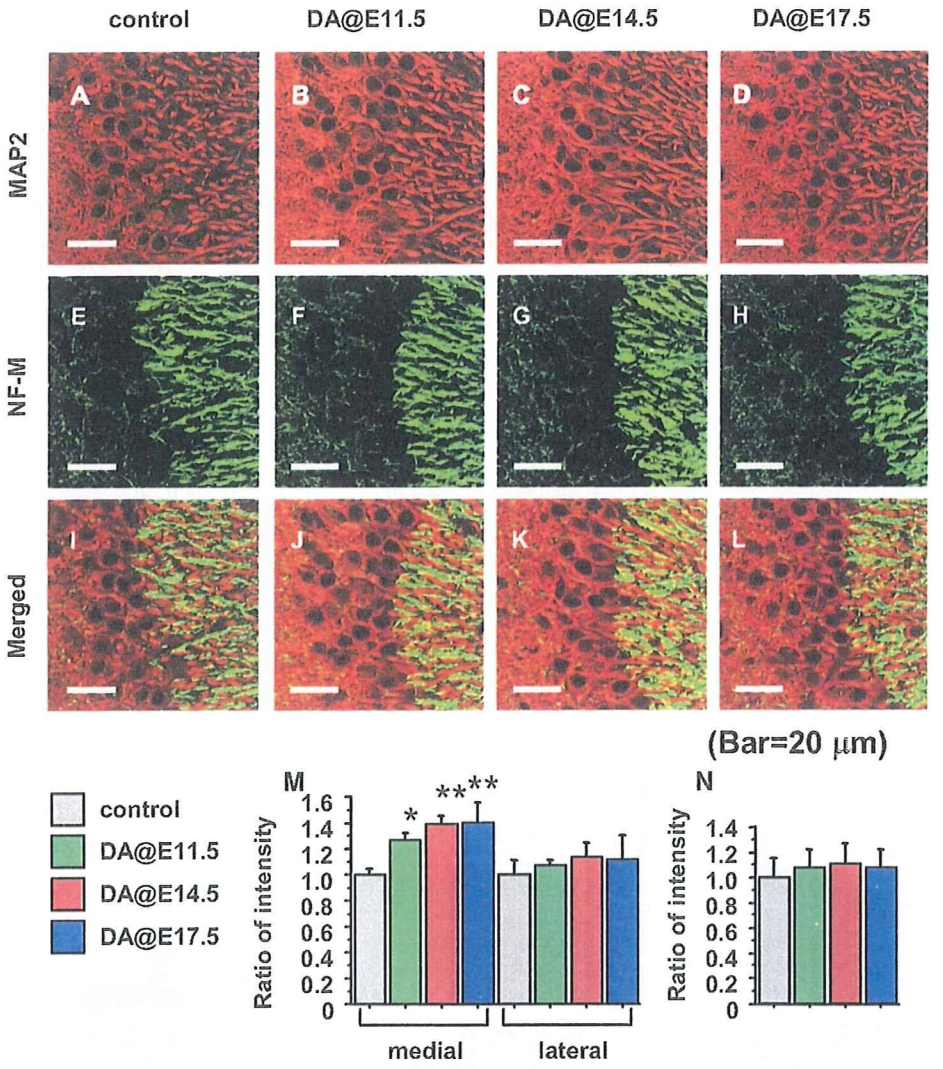

Fig. 2. Delayed effects on hippocampus induced by prenatal exposure of DA.
A-D, Immunohistochemical staining against MAP2; E-H, immunohistochamical staining against NF-M; I-L, merged images, of CA3 hippocampus. A, E, I, group A (control), B, F, J, group B (DA@11.5), C, G, K, group C (DA@14.5) and D, H, L, group D (DA@17.5). Scale bar = 200 mm. M, Quantitative analysis of MAP2 expression, and N, NF-M expression among the groups (mean ± S.E.M.). Asterisk (**) and (*) indicated significant difference compared to control ($P < 0.01$) and ($P < 0.05$).

ing maturation, such as hyperreactivity to handling and to cage mates, and did not present overt malformation of the brain detectable by the routine H&E histology at the age of 2 weeks (data not shown). It is also noted that the spectrum of the neurobehavioral symptoms induced in mice exposed to DA at adulthood was different from those monitored in this study (data not shown).

Although progressive hippocampal neuronal damages were reported to be induced by prenatal administration of DA (0.6 mg/kg intravenous injection to the dam) (Dakshinamurti *et al.*, 1993), we did not find notable neuronal loss or neuronal cell death as the delayed effects in adult mouse brain by prenatal exposure. On the other hand, we found myelination failure (Miller and Mi, 2007) in cortex of group B (DA@11.5) and C (DA@14.5) mice. And we also detected a finding compatible with the overgrowth of neuronal processes in cortex and hippocampus of group B (DA@11.5), C (DA@14.5) and D (DA@14.5)

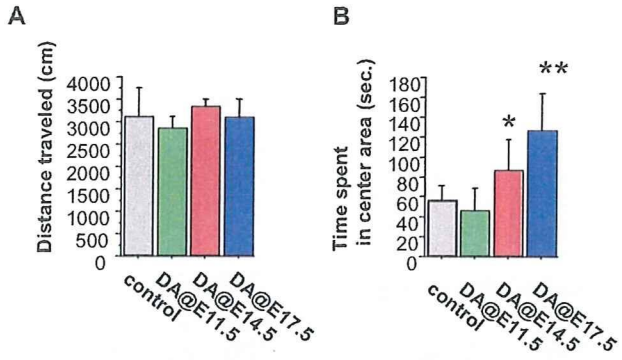

Fig. 3. Delayed effects on locomotor activity (OF test) induced by prenatal exposure of DA.
A, Mean distance travelled (total distances divided by total duration of trial, 10 min) and B, mean time spent in center area (30% of the field) in the open field apparatus (mean ± S.E.M.). Asterisk (**) and (*) indicated significant difference compared to control ($P < 0.01$) and ($P < 0.05$).

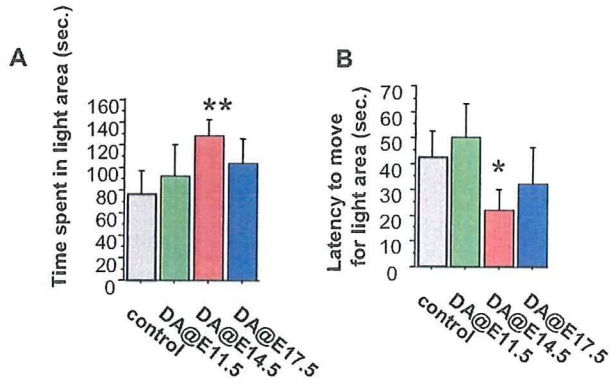

Fig. 4. Delayed effects on anxiety-related behavior (LD test) induced by prenatal exposure of DA.
A, Total time spent in light area, and B, latency time to move to light area in the LD apparatus (mean ± S.E.M.). Asterisk (**) and (*) indicated significant difference compared to control ($P < 0.01$) and ($P < 0.05$).

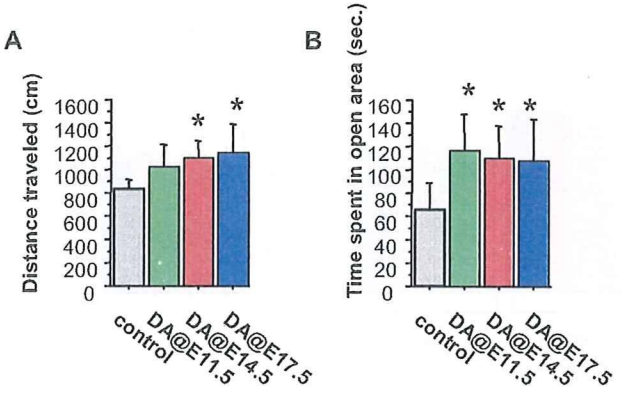

Fig. 5. Delayed effects on anxiety-related behavior (EP test) induced by prenatal exposure of DA.
A, Total distance travelled, and B, total time spent in open area in the elevated plus maze apparatus (mean ± S.E.M.). Asterisk (*) indicated significant difference compared to control ($P < 0.05$).

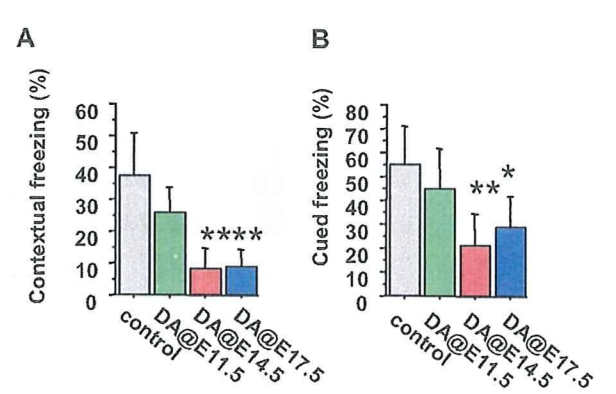

Fig. 6. Delayed effects on learning and memory (FZ test) induced by prenatal exposure of DA.
A, Contextual fear test and B, cued fear test. Memory performance is expressed as a mean percent duration of freezing responses (mean ± S.E.M.). Asterisk (**) and (*) indicated significant difference compared to control ($P < 0.01$) and ($P < 0.05$).

mice by using cytoskeletal marker. These findings indicated that the disorganization of brain was induced by the prenatal exposure of DA, and remained irreversibly up until the maturation period.

Among multiple endpoints of the behavioral test battery we used, serious deviances in anxiety-related behaviors of group C (DA@14.5) and D (DA@17.5) mice were observed. Mice in those groups showed low performances in adaptations for novel circumstances, i.e., strange and broad area in OF test, beamish place in LD test, high and narrow space in EP test. Additionally, we also found severe impairment of learning and memory. Although the low performances of memory task have been reported in rats with prenatal DA exposure (Levin *et al.*, 2005),

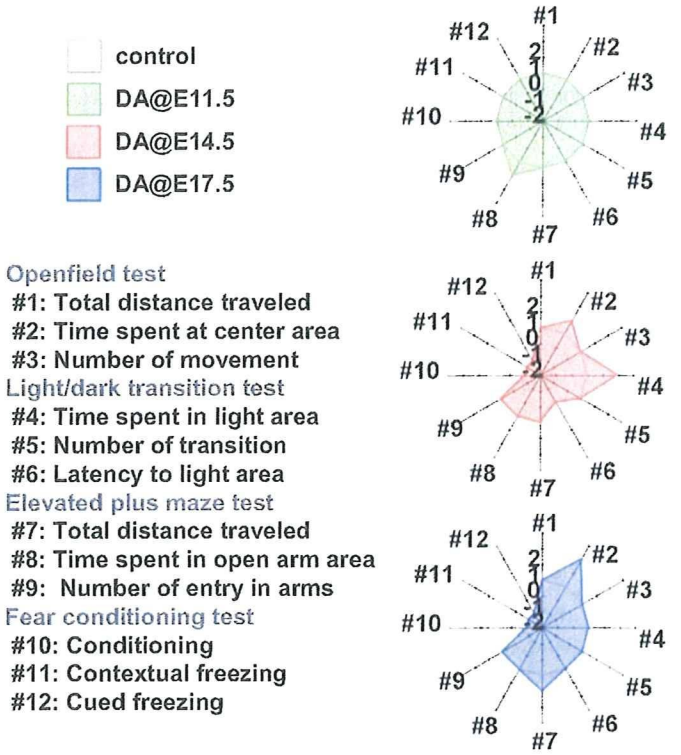

Fig. 7. Summary radar chart of the neurobehavioral battery test results. Radial axis indicates the direction (increase or decrease) of the deviation, and the p value of the endpoints compared to the control (+1 and −1, $0.01 <= p < 0.05$, +2 and −2, $p < 0.01$). Regular dodecagon of radius 0 indicates no deviation from control.

we showed serious deviances about affective (emotional) behaviors additional to severe memory deficit.

In conclusion, we clearly indicated that the disturbance against the adequate neural activity during developmental period when glutamate receptors became active have induced delayed memory defect and unnatural adoptive behaviors that became monitorable at the maturation period in mice. The responsible foci deduced from these behavioral disturbances are the limbic cortex and hippocampus. Our morphological findings are consistent with the interpretation. A combination of neurobehavioral and pathomorphological analysis was shown to be an effective method to assess delayed neurotoxic effects which dose not induce immediate organic brain damage and related symptoms after exposure. Having adopted the hypothesis that exogenous stimuli to neural signaling systems during the development of the brain can be a cause of delayed anomaly of higher brain function, stimuli toward systems other than glutamate receptors should also induce such anomaly of different targets and symptoms in concert with the distribution of the corresponding receptor(s) in the developing brain. Such data on other system would be reported elsewhere.

ACKNOWLEDGMENTS

The authors thank Mr. Yusuke Furukawa and Ms. Maki Otsuka for technical support. This study was supported by Health Sciences Research Grants H17- -Kagaku- 001 from the Ministry of Health, Labour and Welfare, Japan.

This peer-reviewed article is based upon a lecture presented at the 35th Annual Meeting of Japanese Society of Toxicology, June 2008 in Tokyo under the theme of "Children's Toxicology", June 2008 in Tokyo.

REFERENCES

Bondy, S.C. and Campbell, A. (2005): Developmental neurotoxicology. J. Neurosci. Res., **81**, 605-612.

Chandrasekaran, A., Ponnambalam, G. and Kaur, C. (2004): Domoic acid-induced neurotoxicity in the hippocampus of adult rats. Neurotox. Res., **6**, 105-117.

Cohen-Cory, S. (2002): The developing synapse: construction and

modulation of synaptic structures and circuits. Science, **298**, 770-776.

Dakshinamurti, K., Sharma, S.K., Sundaram, M. and Watanabe, T. (1993): Hippocampal changes in developing postnatal mice following intrauterine exposure to domoic acid. J. Neurosci., **13**, 4486-4495.

Fonta, C., Chappert, C. and Imbert, M. (2000): Effect of monocular deprivation on NMDAR1 immunostaining in ocular dominance columns of the marmoset Callithrix jacchus. Vis. Neurosci., **17**, 345-352.

Greer, P.L. and Greenberg, M.E. (2008): From synapse to nucleus: calcium-dependent gene transcription in the control of synapse development and function. Neuron, **59**, 846-860.

Gu, Q.A., Bear, M.F. and Singer, W. (1989): Blockade of NMDA-receptors prevents ocularity changes in kitten visual cortex after reversed monocular deprivation. Brain Res. Dev. Brain Res., **47**, 281-288.

Levin, E.D., Pizarro, K., Pang, W.G., Harrison, J. and Ramsdell, J.S. (2005): Persisting behavioral consequences of prenatal domoic acid exposure in rats. Neurotoxicol. Teratol., **27**, 719-725.

Luján, R., Shigemoto, R. and López-Bendito, G. (2005): Glutamate and GABA receptor signalling in the developing brain. Neuroscience, **130**, 567-580.

Manent, J.B., Demarque, M., Jorquera, I., Pellegrino, C., Ben-Ari, Y., Aniksztejn, L. and Represa, A. (2005): A noncanonical release of GABA and glutamate modulates neuronal migration. J Neurosci., **25**, 4755-4765.

Matsugami, T.R., Tanemura, K., Mieda, M., Nakatomi, R., Yamada, K., Kondo, T., Ogawa, M., Obata, K., Watanabe, M., Hashikawa, T. and Tanaka, K. (2006): Indispensability of the glutamate transporters GLAST and GLT1 to brain development. Proc. Natl. Acad. Sci. USA, **103**, 12161-12166.

Maucher, J.M. and Ramsdell, J.S.(2007): Maternal-fetal transfer of domoic acid in rats at two gestational time points. Environ Health Perspect., **115**, 1743-1746.

Miller, R.H. and Mi, S. (2007): Dissecting demyelination. Nat. Neurosci., **10**, 1351-1354.

Ooi, L. and Wood, I.C. (2008): Regulation of gene expression in the nervous system. Biochem. J., **414**, 327-341.

Pulido, O.M. (2008): Domoic acid toxicologic pathology: a review. Mar. Drugs, **6**, 180-219.

Rice, D. and Barone, S.Jr. (2000): Critical periods of vulnerability for the developing nervous system: evidence from humans and animal models. Environ. Health Perspect., **108**, 511-533.

Tanemura, K., Murayama, M., Akagi, T., Hashikawa, T., Tominaga, T., Ichikawa, M., Yamaguchi, H. and Takashima, A. (2002): Neurodegeneration with tau accumulation in a transgenic mouse expressing V337M human tau. J Neurosci., **22**, 133-141.

Tanemura, K., Ogura, A., Cheong, C., Gotoh, H., Matsumoto, K., Sato, E., Hayashi, Y., Lee, H.W. and Kondo, T. (2005): Dynamic rearrangement of telomeres during spermatogenesis in mice. Dev. Biol., **281**, 196-207.

Tatebayashi, Y., Miyasaka, T., Chui, D.H., Akagi, T., Mishima, K., Iwasaki, K., Fujiwara, M., Tanemura, K., Murayama, M., Ishiguro, K., Planel, E., Sato, S., Hashikawa, T. and Takashima, A. (2002): Tau filament formation and associative memory deficit in aged mice expressing mutant (R406W) human tau. Proc. Natl. Acad. Sci. USA, **99**, 13896-13901.

Tryphonas, L. and Iverson, F. (1990): Neuropathology of excitatory neurotoxins: the domoic acid model. Toxicol Pathol., **18**, 165-169.

Wiesel, T.N. (1982): Postnatal development of the visual cortex and the influence of environment. Nature, **299**, 583-591.

Neonatal Exposure to Low-Dose 2,3,7,8-Tetrachlorodibenzo-*p*-Dioxin Causes Autoimmunity Due to the Disruption of T Cell Tolerance[1]

Naozumi Ishimaru,* Atsuya Takagi,† Masayuki Kohashi,* Akiko Yamada,* Rieko Arakaki,* Jun Kanno,† and Yoshio Hayashi[2]*

Although 2,3,7,8-tetrachlorodibenzo-*p*-dioxin (TCDD) has been shown to influence immune responses, the effects of low-dose TCDD on the development of autoimmunity are unclear. In this study, using NFS/*sld* mice as a model for human Sjögren's syndrome, in which the lesions are induced by the thymectomy on day 3 after birth, the autoimmune lesions in the salivary glands, and in later phase, inflammatory cell infiltrations in the other organs were developed by neonatal exposure to nonapoptotic dosage of TCDD without thymectomy on day 3 after birth. We found disruption of thymic selection, but not thymic atrophy, in TCDD-administered mice. The endogenous expression of aryl hydrocarbon receptor in the neonatal thymus was significantly higher than that in the adult thymus, suggesting that the neonatal thymus may be much more sensitive to TCDD compared with the adult thymus. In addition, the production of T_H1 cytokines such as IL-2 and IFN-γ from splenic $CD4^+$ T cells and the autoantibodies relevant for Sjögren's syndrome in the sera from TCDD-exposed mice were significantly increased compared with those in control mice. These results suggest that TCDD/aryl hydrocarbon receptor signaling in the neonatal thymus plays an important role in the early thymic differentiation related to autoimmunity. *The Journal of Immunology,* 2009, 182: 6576–6586.

The toxicity of 2,3,7,8-tetrachlorodibenzo-*p*-dioxin (TCDD),[3] the environmental contaminant, has been shown to influence various biological responses such as immunological, reproductive, and neurobehavioral (1–3). It has been reported that TCDD induces thymic atrophy and suppresses a variety of T cell-dependent immune responses, including delayed-type and contact hypersensitivity responses and the activity of CTL itself (4–7). However, TCDD has been shown to enhance the proliferation and cytokine production of mitogen- or Ag-stimulated T cells (8). In this context, when a DO11.10 transgenic T cell model was used to investigate the effects of TCDD on the activation of Ag-specific $CD4^+$ T cells by transfer of $CD4^+$ T cells into TCDD-treated recipient mice, the exposure to TCDD had little effect on the initial activation, but on day 3 after OVA-peptide injection the T cell proliferation of TCDD-treated recipients was enhanced compared with that of control recipients (9). Thus, the effect of TCDD seems to be dependent on the developmental state and active state of the T cells. As for the effects of TCDD on B cells, it was reported that TCDD inhibited B cell proliferation triggered by LPS, surface Ig cross-linking, or PMA/ionomycin (10, 11). Moreover, the in vivo suppressive effect of TCDD on T cell-dependent Ab response to sheep RBC (SRBC) was found as an immunotoxicity of TCDD (12). However, the effects of TCDD on autoimmunity or on autoantibody production in autoimmune animal models have not been demonstrated.

A combination of immunologic, genetic, and environmental factors may play a key role on the development of autoimmune disease, which is induced by the breakdown of central or peripheral tolerance (13–15). Sjögren's syndrome (SS) is generally considered to be a T cell-mediated autoimmune disorder characterized by lymphocytic infiltrates and destruction of the exocrine glands, particularly of the salivary glands, and systemic production of autoantibodies against the ribonucleoprotein particles SS-A/Ro and SS-B/La (16–18). We have established and analyzed an animal model for SS in NFS/*sld* mutant mouse thymectomized 3 days after birth (3d-Tx) (19–21). It is well established that 3d-Tx in a certain strain of mice results in spontaneous development of inflammatory lesions similar to human autoimmune diseases in the thyroid, ovary, kidney, testis, and stomach, but little is known about the mechanisms leading to the induction of autoimmunity (22–25). From the findings in 3d-Tx autoimmune models, the initiation of autoreactivity is thought to be due to the retardation of regulatory T (Treg) cell differentiation together with lymphopenia caused by neonatal thymectomy. In other words, the impairment of T cell differentiation and/or maturation in the neonatal thymus may cause the initiation of T cell self-reactivity. Although the perinatal exposure to TCDD has been shown to induce the suppression of cell-mediated immunity to a more severe degree than those in adult exposure, the association of neonatal exposure to TCDD with the development of autoimmunity remains unclear (5, 6).

*Department of Oral Molecular Pathology, Institute of Health Biosciences, University of Tokushima Graduate School, Kuramotocho, Tokushima, Japan; and †Division of Cellular and Molecular Toxicology, Biological Safety Research Center, National Institute of Health Sciences, Kamiyoga, Setagayaku, Tokyo, Japan

Received for publication July 14, 2008. Accepted for publication March 17, 2009.

The costs of publication of this article were defrayed in part by the payment of page charges. This article must therefore be hereby marked *advertisement* in accordance with 18 U.S.C. Section 1734 solely to indicate this fact.

[1] This work was supported by a Health Sciences Research Grant (H17, 18, and 19-kagaku-ippan-003) from the Ministry of Health, Labor and Welfare, Japan and a Grant-in-Aid for Scientific Research (no. 17109016) from the Ministry of Education, Culture, Sports, Science and Technology of Japan.

[2] Address correspondence and reprint requests to Dr. Yoshio Hayashi, Department of Oral Molecular Pathology, Institute of Health Biosciences, University of Tokushima Graduate School, 3-18-15 Kuramotocho, Tokushima 770-8504, Japan. E-mail address: hayashi@dent.tokushima-u.ac.jp

[3] Abbreviations used in this paper: TCDD, 2,3,7,8-tetrachlorodibenzo-*p*-dioxin; 3d-Tx, thymectomized 3 days after birth; AhR, aryl hydrocarbon receptor; AIRE, autoimmune regulator; ARNT, AhR nuclear translocator; DN, double negative; DP, double positive; DRE, dioxin responsive element; IRF, IFN regulatory factor; SP, single positive; SS, Sjögren's syndrome; TEC, thymic epithelial cell; Treg, regulatory T; XRE, xenobiotic response element.

www.jimmunol.org/cgi/doi/10.4049/jimmunol.0802289

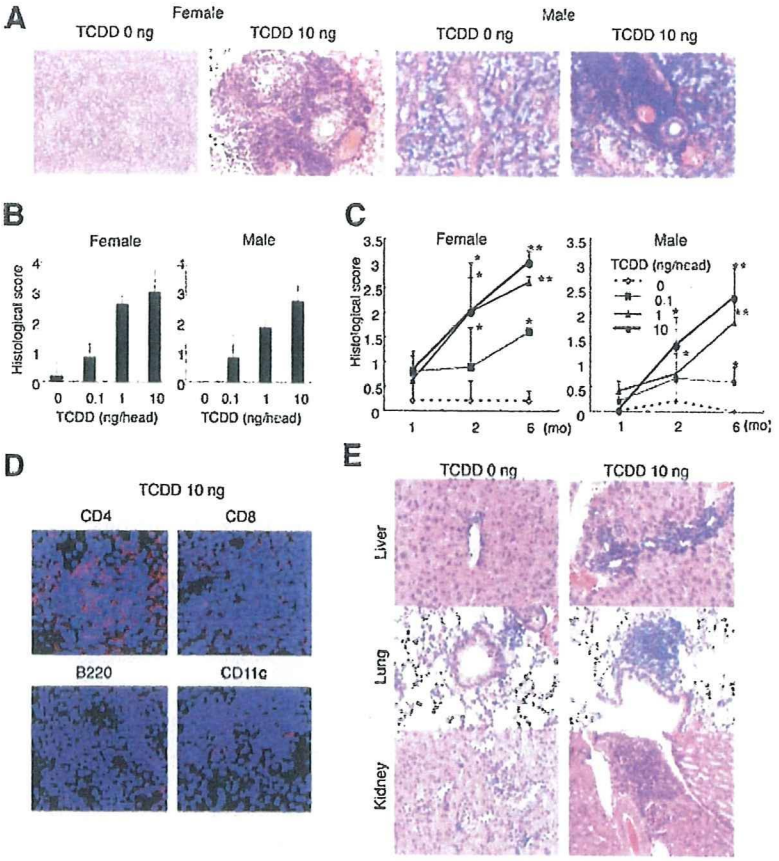

FIGURE 1. Inflammatory lesions induced by neonatal exposure to low-dose TCDD. *A*, Histology of salivary glands in female and male mice (6 mo) treated with 0 and 10 ng of TCDD were shown. H&E staining was performed using paraffin-embedded sections. Photos are representative of five to seven mice in each group. *B*, Histological score of the salivary glands at 6 mo of age was evaluated using the sections stained with H&E. Results are shown as the mean ± SD in the five to seven mice in each group. *C*, The change of inflammatory lesions from 1 to 6 mo of age in female and male mice treated with low-dose TCDD. Results are shown as the mean ± SD in the five to seven mice in each group. *, $p < 0.05$; **, $p < 0.005$. *D*, Immune cells in the inflammatory lesions of salivary glands from TCDD-treated mice at 6 mo of age were analyzed by immunofluorescence staining using anti-CD4, CD8, B220, and CD11c mAbs with Alexa Fluor 568-conjugated rat IgG (H+L) as the secondary Abs. Nuclei were stained with 4′,6-diamidino-2-phenylindole. Photos are representative of three to five sections in each group. *E*, Inflammatory lesions of liver, lung, and kidney induced by TCDD treatment. The sections from TCDD-treated mice at 6 mo of age were stained with H&E. Photos are representative of five to seven mice in each group.

One mechanism of TCDD action is binding and activation of the aryl hydrocarbon receptor (AhR) (1, 26). The AhR is a cytosolic transcription factor of the basic helix-loop-helix family. The activated receptor heterodimerizes with the AhR nuclear translocator (ARNT) in the nucleus and binds the xenobiotic response elements (XREs), also known as dioxin responsive elements (DREs), and alters the expressions of various genes such as cytochrome P450 1A1 (CYP1A1). TCDD, via the AhR, has been shown to have a variety of effects on T cell development and function, including decreasing the number of thymocytes by apoptosis and altering the effector functions of mature Th and T killer cells (27–30). Although a variety of studies have been performed to determine how high-dose TCDD is influencing T cells and the thymus (29–31), the mechanism and targets of its actions are still unclear. In addition, TCDD also induced the binding of several NF-κB proteins to a κB site, one of which overlapped with a DRE site (32). It has been uncertain whether the neonatal exposure to low-dose TCDD in vivo influences the TCDD signaling including AhR, CYP1A1, or NF-κB of immune cells.

In this study, we evaluated whether the immunotoxicity of nonapoptotic and low-dose TCDD during neonatal period influences the development of autoimmune disease in the murine SS-susceptible strain. Moreover, the correlation between the TCDD-induced signaling pathway in neonatal T cells and the initiation of self-reactivity in vivo was analyzed.

Materials and Methods

Mice

NFS/N strain carrying the mutant gene *sld* was reared in our specific pathogen-free mouse colony, and given food and water ad libitum. Experiments were humanely conducted under the regulation and permission of the Animal Care and Use Committee of the National Institute of Health Sciences, Tokyo, Japan and the University of Tokushima, Tokushima, Japan.

Neonatal administration of TCDD

Intraperitoneal injection of 10 μl of corn oil including TCDD (0, 0.1, 1, or 10 ng/mouse) with neonatal mice was performed on day 0, 1, and 2 after birth. Treatment of TCDD and TCDD-injected mice followed the rules of the National Institute of Health Sciences.

Histology

All organs were removed from the mice, fixed with 4% phosphate-buffered formaldehyde (pH 7.2), and prepared for histologic examination. Formalin-fixed tissue sections were subjected to H&E staining, and three pathologists independently evaluated the histology without being informed of the condition of each individual mouse. Histological changes were scored according to the method proposed by White and Casarett (33), as follows: 1 = 1–5 foci composed of >20 mononuclear cells per focus; 2 = >5 such foci, but without significant parenchymal destruction; 3 = degeneration of parenchymal tissue; 4 = extensive infiltration of the glands with mononuclear cells and extensive parenchymal destruction. Histological evaluation was performed in a blinded manner, and one tissue section from each salivary and lacrimal gland was examined.

Confocal microscopic analysis

Frozen sections were stained with 1 μg/ml primary Abs against CD4, CD8, B220, and CD11b/c (eBioscience) for 1 h. After three washes in PBS, the sections were stained with Alexa Fluor 568 donkey anti-rat IgG (H+L) (Molecular Probes) as the second Abs for 30 min and washed with PBS. The nuclei was stained with 4′,6-diamidino-2-phenylindole. The sections were visualized with a laser scanning confocal microscope (Carl Zeiss). A 63 × 1.4 oil differential interference contrast objective lens was used. Quick Operation Version 3.2 (Carl Zweiss) for imaging acquisition and Adobe Photoshop CS2 (Adobe System) for image processing was used.

Table I. *Incidence of inflammatory lesions in TCDD-treated mice*

	Female			Male		
	1 mo	2 mo	6 mo	1 mo	2 mo	6 mo
Liver treated with TCDD (ng)						
0	0/5 (0)	0/7 (0)	0/5 (0)	0/6 (0)	0/6 (0)	0/9 (0)
0.1	0/6 (0)	2/8 (25)	2/5 (40)	0/5 (0)	0/6 (0)	2/6 (33)
1	1/5 (20)	2/6 (33)	1/6 (17)	4/8 (50)	0/6 (0)	2/6 (33)
10	2/5 (40)	3/6 (50)	2/6 (33)	2/6 (33)	4/6 (67)	5/7 (71)
Lung treated with TCDD (ng)						
0	0/5 (0)	0/7 (0)	1/6 (17)	0/6 (0)	0/7 (0)	0/9 (0)
0.1	0/6 (0)	4/8 (50)	3/5 (60)	0/5 (0)	0/5 (0)	3/6 (50)
1	1/5 (20)	2/6 (33)	4/6 (67)	2/8 (25)	3/6 (50)	6/6 (100)
10	2/5 (40)	3/6 (50)	6/6 (100)	1/6 (17)	6/6 (100)	7/7 (100)
Kidney treated with TCDD (ng)						
0	0/5 (0)	0/7 (0)	0/6 (0)	0/6 (0)	0/7 (0)	0/9 (0)
0.1	0/6 (0)	0/8 (0)	1/5 (20)	1/5 (20)	3/5 (60)	4/6 (67)
1	0/5 (0)	0/6 (0)	2/6 (33)	2/8 (25)	4/6 (67)	5/6 (83)
10	1/5 (20)	3/6 (50)	2/6 (33)	2/6 (33)	6/6 (100)	5/7 (71)

The incidence of inflammatory lesions in the liver, lung, and kidney was histologically evaluated using the H&E-stained sections of the TCDD-treated NFS/*sld* mice at 1, 2, and 6 mo of age. The number of inflammatory lesion-induced mice in the organ/the total number of treated mice (%) is indicated.

Flow cytometric analysis

Surface markers were identified by mAbs with BD FACSCant flow cytometer (BD Biosciences). Rat mAbs to FITC-, PE-, or PE-Cy5-conjugated anti-B220, Thy1.2, CD4, CD8, CD25, and CD44 mAbs (eBioscience) were used. Intracellular Foxp3 expression was analyzed with an intracellular Foxp3 detection kit (eBioscience) according to the manufacturer's instructions. For intracellular AhR expression, cells were stained with PE-Cy5.5-conjugated anti-CD4, PE-conjugated anti-CD8, PE-Cy7-conjugated anti-CD44, allophycocyanin-conjugated anti-CD25 mAbs, and then fixed in fixation/permeabilization solution (eBioscience) for 18 h at 4°C. After washing twice with the permeabilization buffer (eBioscience), the cells were blocked with Fc block for 40 min on ice, and incubated in rabbit anti-AhR polyclonal Ab (BIOMOL) for 2 h at 4°C. After washing with the permeabilization buffer, the cells were stained with FITC-conjugated ant-rabbit IgG for 30 min at 4°C for flow cytometric analysis of multicolors. The data were analyzed with FlowJo FACS Analysis software (Tree Star).

Proliferation assay

Cell proliferation was evaluated by counting of divisions by CFSE (Molecular Probes) dilution of labeled cells. After stimulation by anti-CD3 and

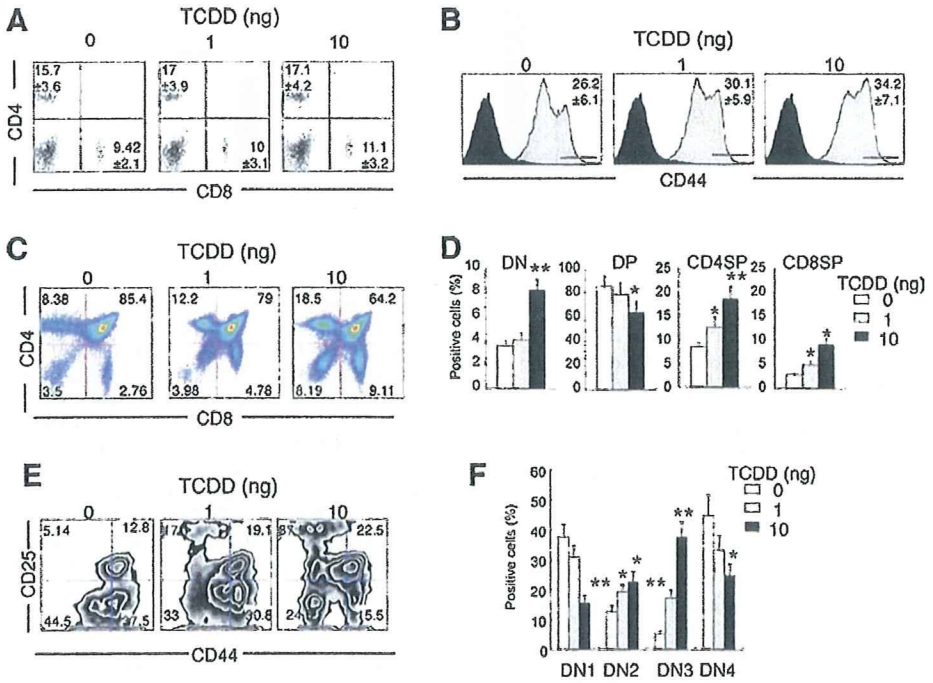

FIGURE 2. The effect of in vivo TCDD injection on T cell phenotypes. *A*, CD4 and CD8 expressions on spleen cells from female TCDD-treated mice at 6 mo of age were analyzed by flow cytometry. Positive cells (%) were indicated as the mean ± SD of five to seven mice in each group. *B*, CD44 expression on $CD4^+$ T cells in spleen from TCDD-treated mice. $CD44^{high}$ cells (%) are indicated as the mean ± SD of five to seven mice in each group. *C*, T cell differentiation in thymus of TCDD-treated mice was analyzed by flow cytometry using CD4 and CD8 expressions. Figures are representative of five to seven mice in each group. *D*, T cell population in thymus. $CD4^-CD8^-$ DN, $CD4^+CD8^+$ DP, $CD4^+CD8^-$ SP (CD4SP), and $CD4^-CD8^+$ SP (CD8SP) cells (%) are shown as the mean ± SD of five to seven mice in each group. *E*, The differentiation of DN T cells was evaluated using CD44 and CD25 expressions. Figures are representative of five to seven mice in each group. *F*, $CD44^+CD25^-$ (DN1), $CD44^+CD25$ (DN2), $CD44^-CD25^+$ (DN3), and $CD44^-CD25^-$ (DN4) cells (%) are shown as the mean ± SD of five to seven mice in each group. *, $p < 0.05$; **, $p < 0.005$.

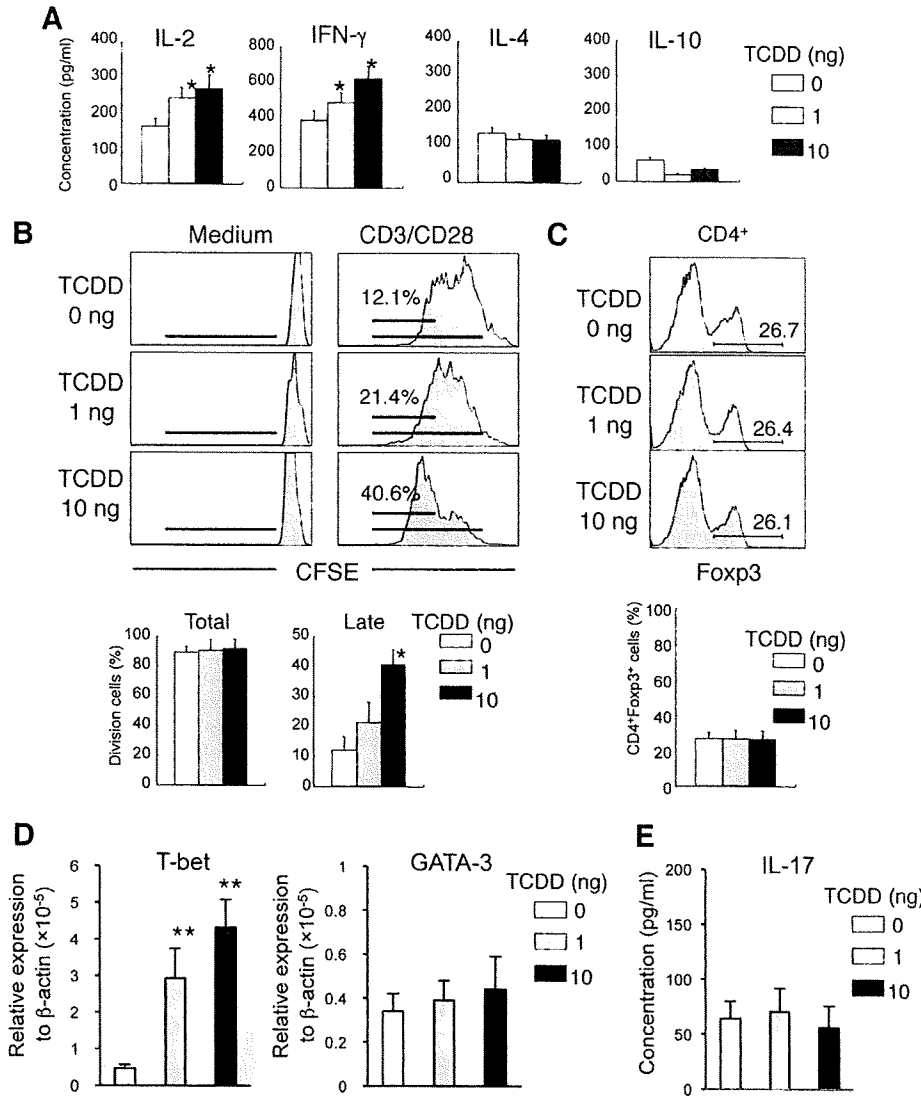

FIGURE 3. T cell functions in low-dose TCDD-treated mice. *A*, T_H1 and T_H2 type cytokine productions were analyzed by ELISA using the culture supernatants from splenic T cell-stimulated plate-coated anti-CD3 mAb for 24 h. Results are shown as mean ± SD of triplicates and representative of four to five mice in each group. *B*, Proliferative response of splenic T cell-stimulated plate-coated anti-CD3 and CD28 mAbs from TCDD-treated mice was analyzed with CFSE dilutions during 72 h. Results are representative of three to five mice in each group. *C*, $Foxp3^+CD4^+$ Treg cells in spleen from TCDD-treated mice were analyzed by flow cytometry. Results are representative of three to five mice in each group. $Foxp3^+$ cells (%) are indicated as mean ± SD of three to five mice in each group. *, $p < 0.05$. *D*, T-bet and GATA-3 mRNA expressions of spleen from TCDD-treated mice were detected by real-time PCR. Data are shown as mean ± SD of four to six mice per each group. *, $p < 0.05$; **, $p < 0.005$. *E*, IL-17 production was analyzed by ELISA using the culture supernatants from splenic T cell-stimulated plate-coated anti-CD3 mAb for 24 h. Results are shown as mean ± SD of triplicates and representative of four mice in each group.

anti-CD28 mAbs, or LPS for 72 h, cell division of $CD4^+$ or $B220^+$-gated spleen cells was analyzed by flow cytometry.

ELISA

The JS-1-, SS-A/Ro-, SS-B/La-, or ss-DNA-specific Abs of sera from mice were measured by an ELISA reader (model 680; Bio-Rad) with a spectrophotometer reading at 490 nm. Igs (IgG2a and IgG1) in sera were determined by using the mouse immunoglobulins ELISA quantitation kit (Bethyl Laboratories). For detection of IL-2, IFN-γ, IL-4, IL-10, and IL-17 in the culture supernatants from anti-CD3 mAb-stimulated splenic $CD4^+$ T cells for 24 h, ELISA were performed by using each specific Ab for the cytokines as previously described (34).

Real-time quantitative RT-PCR

Total RNA was extracted from thymus, spleen, and cultured thymocytes in NFS/*sld* mice using Isogen (Wako Pure Chemical), and reverse transcribed. Transcript levels of T-bet, GATA-3, AhR, CYP1A1, Bcl-xL, TNF-α, IFN regulatory factor (IRF)-1, GADD45, IL-1β, autoimmune regulator (AIRE), salivary protein-1, GAD67, and β-actin were performed using DNA Engine OPTICOM system (Bio-Rad) with SYBR Premix Ex Tag (Takara Shuzo). Primer sequences were as follows: T-bet: forward, 5′-CCTGTTGTGGTCCAAGTTCAAC-3′ and reverse, 5′-CACAAACAT CCTGTAATGGCTTGT-3′; GATA-3: forward, 5′-GACTTGCCAGAAAG GCAGAC-3′, and reverse, 5′-AAAGAGGTCACCACCCACAG-3′; AhR: forward, 5′-ACATAACGGACGAAATCCTGACC-3′ and reverse, 5′-TC AACTCTGCACCTTGCTTAGGA-3′; CYP1A1: forward, 5′-CCATGACC GGGAACTGTGG-3′, and reverse, 5′-TCTGGTGAGCATCCTGGACA-3′; NF-κB: forward, 5′-ATGGCAGACGATGATCCCTA-3′ and reverse, 5′-TAGGCAAGGTCAGAATGCAC-3′; Bcl-xL: forward, 5′-AGAAGA AACTGAAGCAGAG-3′, and reverse, 5′-TCCGACTCACCAATACCT G-3′; TNF-α, forward, 5′-ATGAGCACAGAAAGCATGATC-3′, and reverse, 5′-AGATGATCTGAGTGTGAGGG-3′; GADD45: forward, 5′-TG GTGACGAACCCACATTCAT-3′, and reverse, 5′-ACCCACTGATCCAT GTAGCGAC-5′; IL-1β: forward, 5′-TGATGAGAATGACCTGTTCT-3′, and reverse, 5′-CTTCTTCAAAGATGAAGGAAA-3′; AIRE: forward, 5′-AAGGGAGCCCAGGTCACTAT-3′, and reverse, 5′-ATTGAGGAGGGA CTCCAGGT-3′; salivary protein-1: forward, 5′-GGCTCTGAAACTCA GGCAGA-3′, and reverse, 5′-TGCAAACTCATCCACGTTGT-3′; GAD67: forward, 5′-TGCAACCTCCTCGAACGCGG-3′, and reverse, 5′-CCAG GATCTGCTCCAGAGAC-3′; β-actin: forward, 5′-GTGGGCCGCTCT AGGCACCA-3′ and reverse, 5′-CGGTTGGCCTTAGGGTTCAG GGGGG-3′.

NF-κB transcription activity assay

The transcriptional activity of NF-κB of the nuclear extracts from thymocytes was analyzed with NF-κB transcription factor colorimetric assay kit (Millipore). Nuclear extracts were incubated with biotinylated double-strand oligonucleotide probe containing the consensus sequence for NF-κB on a streptavidin-coated plate. Captured complexes, including active NF-κB protein, were incubated with the primary Abs for p50 and RelA and HRP-conjugated secondary Ab and tetramethylbenzidine substrate. The absorbance of the samples was measured with microplate reader at 450 nm.

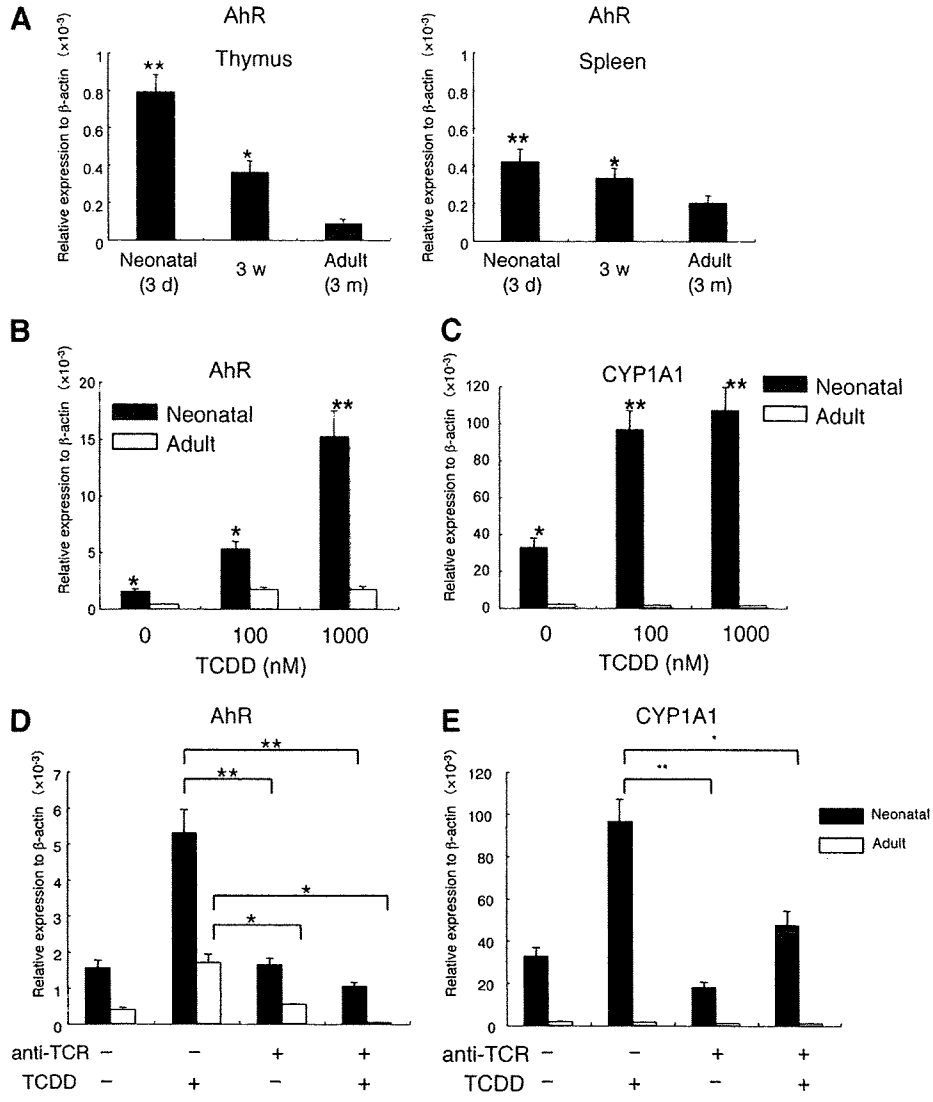

FIGURE 4. Cell signaling through AhR in thymus of NFS/*sld* mice. *A*, Expression of AhR mRNA of thymus and spleen from neonatal and adult NFS/*sld* mice was detected by quantitative RT-PCR. Relative expression to β-actin mRNA is indicated as mean ± SD of four mice in each group. *, $p < 0.05$; **, $p < 0.005$. w, Week. *B* and *C*, For 3 h in 24-well plate, 2×10^6 thymocytes of neonatal and adult NFS/*sld* mice were incubated with 0, 100, and 1000 nM TCDD. The mRNA expressions of AhR (*B*), and CYP1A1 (*C*) were analyzed by quantitative RT-PCR. *D* and *E*, The mRNA expressions of AhR (*D*) and CYP1A1 (*E*) in anti-TCR mAb-stimulated thymocytes from neonatal and adult mice with or without TCDD were detected by quantitative RT-PCR. Data are shown as mean ± SD of triplicate samples. *, $p < 0.05$; **, $p < 0.005$.

Statistical test

The Student *t* test was used for statistical analysis. Values of $p > 0.05$ were considered as significant.

Results

Induction of inflammatory lesions by neonatal administration of low-dose TCDD

To elucidate whether inflammatory lesions are induced by neonatal administration of low-dose TCDD into NFS/*sld* mice, i.p. injection of 0, 0.1, 1, and 10 ng/mouse TCDD was performed on day 0, 1, and 2 after birth. At 1, 2, and 6 mo of age, all the organs of treated mice were histopathologically analyzed. The inflammatory lesions in salivary glands of TCDD-injected mice, similar to those of thymectomized NFS/*sld* mice, were found whereas no lesion was observed in the salivary glands of vehicle-treated mice. The lesions of female mice were more severe than those of male mice (Fig. 1, *A–C*). Lymphocyte infiltration around ducts with destruction of acinar cells was observed in the TCDD-induced lesions (Fig. 1*A*). Severity of the inflammatory lesions was increased in a dose-dependent manner of TCDD (Fig. 1, *B* and *C*). In addition, more severe lesions developed with aging, and observed mainly in female mice (Fig. 1*C*). To characterize the infiltrating immune cells in the inflammatory lesions of salivary glands, the frozen sections were analyzed using the markers of T cells, B cells, and dendritic cells by immunofluorescence staining. $CD4^+$ T cells were mainly infiltrated in the inflammatory lesions of salivary glands from TCDD-treated mice, whereas a small population of $CD8^+$ T cells, B cells, and $CD11c^+$ dendritic cells were seen in the lesions (Fig. 1*D*).

In contrast, the inflammatory lesions of lung, liver, or kidney were also observed in the mice treated with TCDD (Fig. 1*E*). The incidence of the lesions is shown in Table I. At 6 mo of age, slight inflammatory lesions in the liver of 30–50% male mice by 0.1 or 1 ng of TCDD injection were observed. The inflammatory lesions of liver were found in 30–70% of male mice and ~50% of the female mice treated with 10 ng of TCDD at 6 mo of age. Also, the inflammatory lesions of lung with a small number of lymphocyte infiltrates around bronchus or blood vessels were observed in both 100% female and male mice treated with 10 ng of TCDD at 6 mo of age. In addition, the slight inflammation in the kidney from 100% male mice treated with 10 ng of TCDD was observed at 6 mo of age. As for female mice, the renal lesions were found in ~50% of the mice treated with 10 ng of TCDD at 6 mo of age. Induction of inflammatory lesions by TCDD might be dependent on the sex or the sensitivity of each organ, although its precise mechanism is unclear.

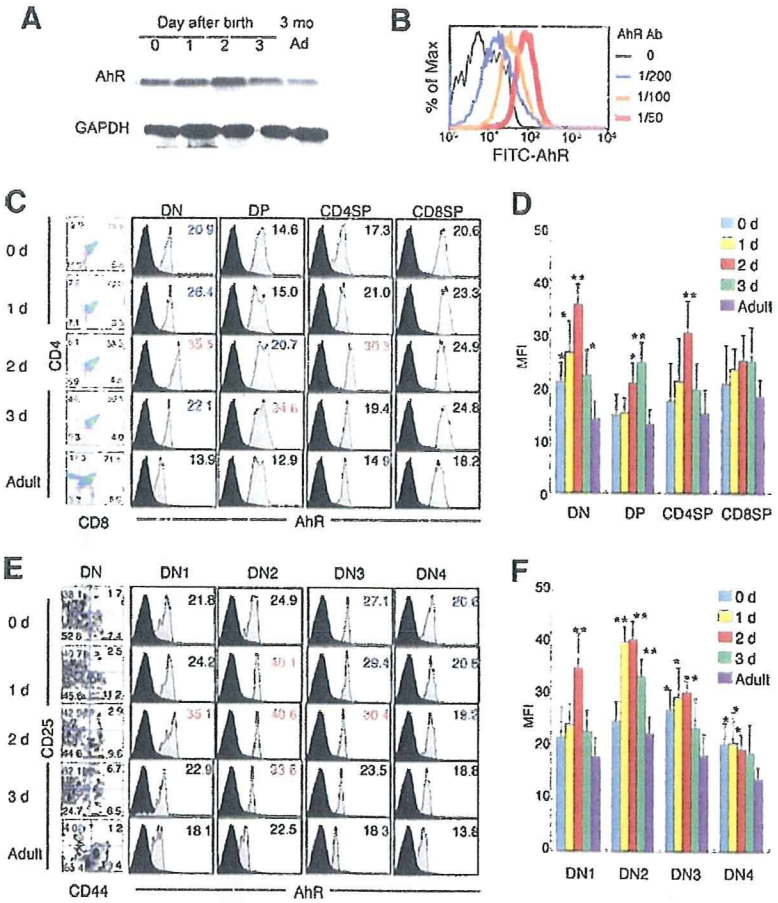

FIGURE 5. Expression of AhR in neonatal thymus. *A*, AhR protein of neonatal thymus from NFS/*sld* mice was detected by Western blotting. Result was representative of two independent experiments. GAPDH expression was used for loading control. *B*, Flow cytometric analysis of intracellular AhR expression. Thymocytes from B6 (3 mo) mice were stained with PE-Cy5.5-CD4 and PE-CD8 mAbs, fixed, washed in perm buffer, and then stained with rabbit anti-AhR Ab and FITC-conjugated anti-rabbit IgG as the second Ab. Diluted anti-AhR Ab (×200, ×100, and ×50) was used for staining. *C* and *D*, Thymocytes from neonatal (days 0, 1, 2, and 3 after birth) and adult (12 wk of age) NFS/*sld* mice were stained with PE-Cy5.5-CD4, PE-CD8, allophycocyanin-CD25, and PE-Cy7-CD44 mAbs, fixed, washed in permeabilization buffer, and then stained with rabbit anti-AhR Ab and FITC-conjugated anti-rabbit IgG as the second Ab. Intracellular AhR expressions of DN, DP, CD4SP, and CD8SP cells in neonatal and adult thymus. Figures are representative of three to four samples. Data are shown as mean ± SD of three to four samples. *E* and *F*, Intracellular AhR expression of DN cells in thymus. Data are shown as mean ± SD of mean fluorescence intensity (MFI) of three to four samples. Colored (blue or red) MFI was indicated in the figure as significantly increased. *, $p < 0.05$; **, $p < 0.005$.

Influence of in vivo low-dose TCDD injection on T cell phenotypes

To examine the influence of neonatal exposure to low-dose TCDD on T cell phenotypes, flow cytometric analysis of the expressions of surface T cell markers was performed on female mice at 6 mo of age (Fig. 2). There was no significant difference in the expression profile of CD4 and CD8 on the spleen cells by treatment of TCDD (Fig. 2*A*). A significantly increased population of memory phenotype, $CD44^{high}CD4^+$ T cell, was observed in the female mice treated with TCDD (Fig. 2*B*). As for thymic maturation, the $CD4^-CD8^-$ double-negative (DN) cells were considerably increased by treatment of 10 ng of TCDD while double-positive (DP) cells significantly decreased by 10 ng of TCDD injection. By contrast, both CD4 single-positive (SP) and CD8SP cells were significantly increased by TCDD injection (Fig. 2, *C* and *D*). Furthermore, when the increased DN cells were analyzed using differentiation markers such as CD25 and CD44, $CD44^+CD25^-$ (DN1) and $CD44^-CD25^-$ (DN4) cells were significantly reduced by in vivo treatment of 10 ng of TCDD, but significantly increased populations of $CD44^+CD25^+$ (DN2) and $CD44^-CD25^+$ (DN3) cells were observed (Fig. 2, *E* and *F*). These results suggested that neonatal exposure to TCDD might influence on thymic differentiation including negative or positive selection of T cells.

The influence of low-dose TCDD on peripheral T cell functions

To know the effect of TCDD on T cell functions in the periphery, cytokine secretions from splenic T cells activated by plate-coated anti-CD3 mAb were analyzed using the culture supernatants by ELISA. T_H1 cytokine production, including IL-2 and IFN-γ from activated T cells of TCDD-treated mice, was significantly increased compared with that of control mice (Fig. 3*A*). By contrast, there was no influence on T_H2 cytokine secretion such as IL-4 and IL-10 by in vivo TCDD injection (Fig. 3*A*). Moreover, proliferative response of splenic T cells stimulated with anti-CD3 and CD28 mAbs was analyzed using CFSE dilutions during 3 days. The cell divisions during the late stage were significantly enhanced by in vivo TCDD injection compared with those of control mice (Fig. 3*B*). In contrast, there was no difference in $Foxp3^+CD25^+CD4^+$ T cells, classical Treg cells, by neonatal TCDD exposure (Fig. 3*C*). It has been known that T-bet for T_H1 and GATA-3 for T_H2 are prime candidates for key transcription factors of each cytokine production of T_H cells (35). T-bet mRNA expression of purified T cells from spleen in TCDD-treated mice was higher than that in control mice. However, there was no change of the GATA-3 mRNA expression by TCDD injection (Fig. 3*D*). In addition, to examine the role of IL-17 in the pathogenesis for TCDD-induced autoimmunity, no change was observed in IL-17 production from anti-CD3 mAb-stimulated T cells of TCDD-treated mice (Fig. 3*E*). These findings show that the neonatal exposure to low-dose TCDD influences on T cell activation or proliferation through enhanced secretion of T_H1 cytokines in the periphery.

Direct influences of TCDD on neonatal thymus

When adult NFS/*sld* mice at 2 mo of age were injected with low-dose TCDD, no inflammatory lesion in any organ was observed until 6 mo of age (our unpublished data). Neonatal exposure to low-dose TCDD may affect the induction of inflammatory lesions in salivary glands resembling the SS model. To evaluate whether

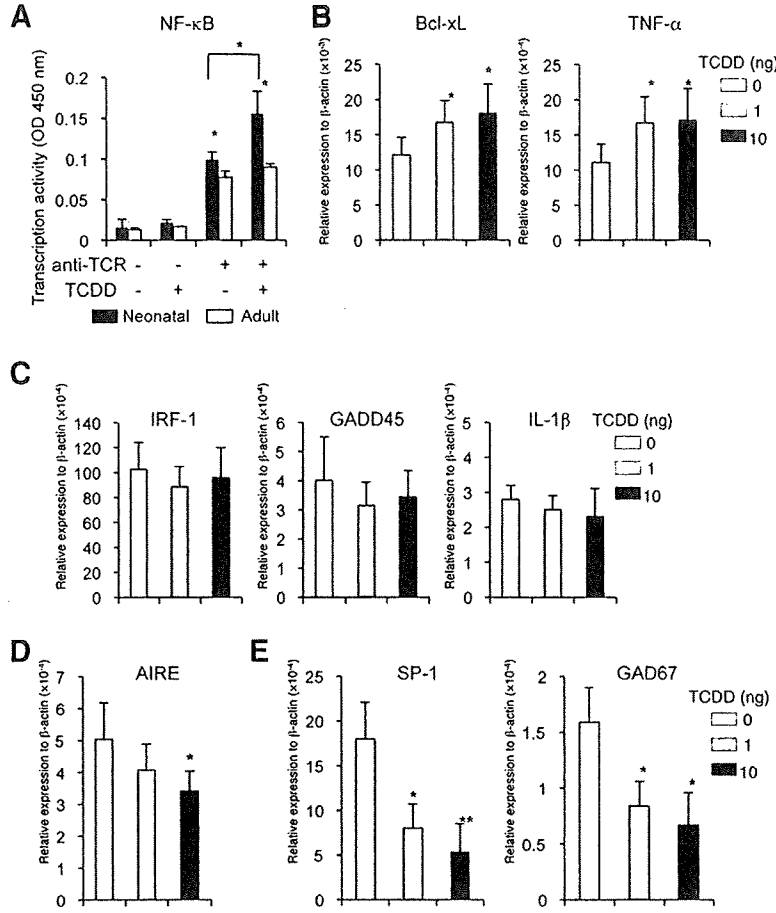

FIGURE 6. Influence of TCDD on central tolerance in thymus. *A*, Transcription activity of NF-κB in thymocytes stimulated with anti-TCR mAb in the presence or absence of TCDD was evaluated. Results are shown as mean ± SD of three samples. *, $p < 0.05$. *B* and *C*, In vivo effect of TCDD on target genes of NF-κB was evaluated to detect the mRNA expressions. The mRNA expressions of NF-κB-regulated genes in thymus tissues from TCDD-treated mice were analyzed by real time-PCR. Results are shown as mean ± SD of four to six mice per each group. *, $p < 0.05$. *D*, AIRE mRNA expression of thymus from TCDD-treated mice. *E*, The mRNA expressions of salivary protein-1 and GAD67 in thymus from TCDD-treated mice. The expressions of thymus from TCDD-treated mice were detected by real-time PCR. *, $p < 0.05$; **, $p < 0.005$.

the exposure to TCDD has much more influence on neonatal thymus compared with adult thymus, the expression of AhR was analyzed by quantitative RT-PCR. Interestingly, in contrast to adult thymus, the expression of AhR mRNA of neonatal thymus from NFS/*sld* mice was much higher (8- to 9-fold) (Fig. 4*A*). The expression was reduced with aging (~3 mo of age). The expression of AhR mRNA in neonatal spleen was higher (2-fold) than that in adult spleen (Fig. 4*A*). Next, to clarify the direct effects of TCDD on thymocytes, neonatal and adult thymocytes were incubated with 0, 100, and 1000 nM TCDD for 3 h to analyze AhR expression. More increased expression of AhR in neonatal thymocytes was observed by TCDD stimulation compared with that in adult thymocytes (Fig. 4*B*). In addition, mRNA expression of CYP1A1, one of target genes for TCDD/AhR/XRE (36), in neonatal thymocytes was much enhanced by TCDD incubation, whereas there was no change in mRNA expression of CYP1A1 in adult thymocytes by TCDD stimulation (Fig. 4*C*). In contrast, there were no significant changes in mRNA expressions of AhR and CYP1A1 of the spleen cells in the response to TCDD between neonatal and adult mice (data not shown). To understand association between TCR and TCDD signaling in thymocytes of neonatal and adult NFS/*sld* mice, plate-coated anti-TCRβ mAb was used for the stimulation of thymocytes with or without TCDD. Up-regulated mRNA expression of AhR by TCDD in both neonatal and adult thymocytes was clearly reduced by stimulation of anti-TCRβ mAb (Fig. 4*D*). In addition, TCDD-induced CYP1A1 mRNA expression in neonatal thymocytes was reduced to the level of non-stimulation by anti-TCRβ mAb (Fig. 4*E*). These findings suggest that neonatal thymocytes may be sensitive to TCDD through highly expressed AhR in NFS/*sld* mice, and that neonatal injection of TCDD might influence thymic differentiation to induce breakdown of tolerance.

Expression of AhR in neonatal thymus

To confirm the higher expression of AhR as a protein in neonatal thymus tissues of NFS/*sld* mice, Western blot analysis was performed. The highest expression of AhR was observed on day 2 after birth, and the expression on day 3 was relatively decreased. The expression in adult (3 mo of age) was lower than that of neonatal thymus (Fig. 5*A*). Next, we tried to detect the intracellular AhR expression in subpopulation of thymocytes by flow cytometric analysis. Flow cytometric analysis showed that most thymocytes clearly expressed AhR in adult (3 mo of age) C57BL/6 mice, and the fluorescence intensity of AhR expression was increased depending on the dose of anti-AhR Ab (Fig. 5*B*). When compared, the AhR expressions at each stage including DN, DP, CD4SP, and CD8SP cells in neonatal thymus of NFS/*sld* mice from day 0 to day 3 after birth with those in adult thymus (3 mo), a significantly increased AhR expression of neonatal (days 0, 1, 2, and 3) DN T cells was observed than that of adult DN cells. In particular, much more AhR expression of DN cells on day 2 was detected during neonatal stage. AhR expression of DP T cells on days 2 and 3 was significantly higher than that of adult DP cells. In contrast, although AhR expression of CD4SP cells on day 2 was significantly higher than that of adult CD4SP cells, there was no change in the expression of AhR of CD8SP cells between neonatal and adult thymus (Fig. 5, *C* and *D*). Furthermore, when the AhR expression of each differentiation stage of DN such as $CD44^+CD25^-$ (DN1), $CD44^+CD25^+$ (DN2), $CD44^-CD25^+$ (DN3), and $CD44^-CD25^-$

(DN4) cells was analyzed, AhR expressions of DN1 cells on day 2, DN2 cells on days 1, 2, and 3, DN3 cells on days 0, 1, and 2, and DN4 cells on days 0, 1, and 2 were significantly higher than those of adult DN cells (Fig. 5, *E* and *F*). Among them, the expressions of neonatal DN2 and DN3 cells were more intensive compared with those of adult thymocytes. In contrast, there was no difference in AhR expression at each stage between neonatal and adult thymocytes from normal B6 mice (data not shown). These findings suggest that AhR expression may be related with development and differentiation of T cells in neonatal thymus of NFS/*sld* mice, and that sensitivity of TCDD in neonates can be explained by the development of autoimmunity through AhR expression.

The influence of exposure to low-dose TCDD on central tolerance

Because higher AhR expression of T cells in neonatal thymus of NFS/*sld* mice was observed (Fig. 5), the cell signal pathway to regulate central tolerance in thymus via TCDD/AhR was analyzed. We focused on NF-κB, one of the responsive factors for TCDD/AhR/XRE signaling (37), which is known to be a key transcription factor for regulation of T cell differentiation, development, and activation (38). When the transcriptional activity of NF-κB in between neonatal and adult thymocytes stimulated with anti-TCR mAb in the presence of TCDD was compared, the neonatal activity was significantly increased relative to that of adult thymocytes (Fig. 6*A*). Also, the NF-κB activity of neonatal thymocytes stimulated with anti-TCR mAb was largely enhanced by the addition of TCDD, whereas the increased activity of adult thymocytes was not observed (Fig. 6*A*). Next, to understand the in vivo cell signaling through NF-κB and TCDD/AhR in thymus, the mRNA levels of NF-κB target genes were analyzed by real-time PCR using the thymus tissues from neonatal TCDD-treated mice. Among them, Bcl-xL and TNF-α mRNAs in thymus tissues from TCDD-treated mice were significantly increased in the dose-dependent manner compared with control mice (Fig. 6*B*). There were no changes to the mRNA expressions of IRF-1, GADD45, IL-1β (Fig. 6*C*), IL-6, inducible NO synthase, and Fas ligand (data not shown) which are target genes of NF-κB for controlling T cell signal.

In contrast, AIRE, an essential transcription factor for the expression of tissue-specific autoantigen in thymic epithelial cells (TECs), is well known to play a key role in T cell differentiation and development related with autoimmunity (39). When AIRE mRNA level in thymus tissues, including TECs from neonatal TCDD-treated NFS/*sld* mice, was analyzed, the expression in 10 ng of TCDD-treated mice was significantly decreased compared with that in control mice (Fig. 6*D*). Moreover, salivary protein-1 and GAD67 are known to be representative for the tissue-specific Ag in salivary gland and pancreas respectively (40). Interestingly, both salivary protein-1 and GAD67 mRNA expressions of the thymus tissues from neonatal TCDD-treated NFS/*sld* mice were significantly reduced relative to those from control mice (Fig. 6*E*). These findings show that neonatal exposure to low-dose TCDD in NFS/*sld* mice might influence the impairment of central tolerance in thymus, resulting in the induction of autoimmune disease.

The influences of low-dose TCDD exposure on B cells

The effects of neonatal exposure to low-dose TCDD on B cell phenotype and function were analyzed (Fig. 7). There was no difference in the number of $B220^+$ B cells from spleen between TCDD-treated and control mice (Fig. 7*A*). Furthermore, no change was observed in the proliferative response of splenic B cells to LPS from TCDD-treated mice compared with that from control mice (Fig. 7*B*). The serum titers of autoantibodies that are associated with SS, including anti-SSA/Ro, anti-SSB/La, and anti-ssDNA, were examined (17, 18). In this study, serum titers of anti-SSA/Ro and anti-SSB/La autoantibodies were significantly increased in TCDD-treated mice at 6 mo of age compared with those in control mice (Fig. 7*C*). It has been reported that thymectomized NFS/*sld* mice and human SS patients have high titers of serum autoantibody against α-fodrin (20, 34). The higher titers of anti-α-fodrin autoantibody in the sera from TCDD-treated mice were also detected from control mice at 6 mo of age (Fig. 7*D*). No significant change for anti-ssDNA was observed between TCDD-treated and control mice (data not shown). In addition, when the ratio of IgG2a and IgG1 that is associated with T_H1 and T_H2 or cellular and humoral immune responses was analyzed using sera from TCDD-injected mice, the ratio from TCDD-injected mice was significantly higher than that from control mice at 6 mo of age (Fig. 7*E*).

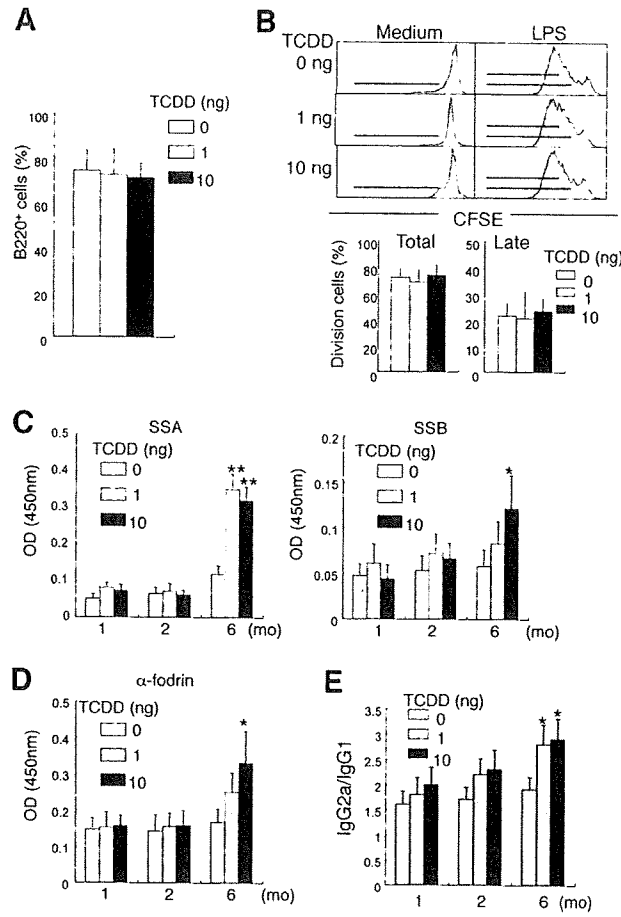

FIGURE 7. Influence on B cell functions by neonatal exposure to low-dose TCDD. *A*, $B220^-$ B cells in spleen from TCDD-treated mice at 6 mo of age were detected by flow cytometric analysis. Results are shown as mean ± SD of five to seven mice in each group. *B*, Proliferative response of splenic B cells stimulated with LPS was evaluated with CFSE dilutions during 72 h. Figures are representative of five to seven mice in each group. *C* and *D*, Serum titers of autoantibodies, including anti-SSA/Ro, anti-SSB/Lo, and anti-α-fodrin from female TCDD-treated mice from 1 to 6 mo of age were measured by ELISA. Results are shown as mean ± SD of five to seven mice in each group. *E*, Ratio of IgG2a/IgG1 in sera from TCDD-injected mice. Serum titer of IgG2a and IgG1 from TCDD-injected NFS/*sld* mice was measured by ELISA. Data are shown as mean ± SD of the ratio from five to seven mice. *, $p < 0.05$; **, $p < 0.005$.

Discussion

TCDD is a widespread environmental contaminant that influences several basic homeostatic control mechanisms in the body via AhR (3). T cells are a possible direct target for TCDD, as evidenced by the presence of the AhR in T cells, and inhibition of T cell growth by the expression of a constitutively active AhR mutant in AhR-null Jurkat T cells or following TCDD treatment (1, 41). It has been demonstrated that expression of AhR in both $CD4^+$ and $CD8^+$ T cells is required for a full suppression of an allospecific CTL response by TCDD, indicating a direct role for AhR in these TCDD-induced immunosuppressive effects (1, 42). However, the relationship between in vivo TCDD exposure and breakdown in T cell tolerance has not been well defined.

In this study, we demonstrated that neonatal exposure to low-dose TCDD could induce autoimmunity in the salivary glands using a NFS/*sld* strain associated with disease-susceptible autoantibody production, such as anti-SSA/La, anti-SSB/Ro, and anti-α-fodrin Abs. It has been reported that TCDD causes extensive damage to the thymus to suppress T cell-dependent immune responses in vivo, including delayed-type and contact hypersensitivity responses and the generation of CTL (4, 43, 44). By contrast, neonatal exposure to TCDD had little influence on thymic atrophy in our experiment in which low-dose (0.0486 ± 0.0088 to 8.37 ± 0.7 μg/kg) TCDD was administered into neonatal mice on days 0, 1, and 2 (body weight: 1.2 ± 0.1 to 2.1 ± 0.35 g) after birth. The dosage of TCDD was considerably lower than that in the experiments in which thymic atrophy or apoptosis was induced by in vivo exposure to TCDD (30–50 μg/kg) (31, 32). For instance, it was reported that 60% apoptotic cells of thymus were observed in normal mice injected with 50 μg/kg TCDD, whereas 20–30% apoptotic cells of thymus were observed in vehicle-injected mice. In addition, although the loss of mitochondrial membrane potential related to apoptosis of thymocytes was not detected in ~10 μg/kg TCDD-treated mice, the loss was observed in 10–50 μg/kg TCDD-treated mice (31). Thus, the exposure to low dosage under 10 μg/kg TCDD may have an influence on neonatal thymic differentiation or selection in NFS/*sld* mice, but not atrophy or apoptosis, to induce autoimmune disease as the late effect. Moreover, T cell proliferation by anti-CD3 and -CD28 mAbs and Th1-type cytokine production, such as IL-2 and IFN-γ from splenic $CD4^+$ T cells, were significantly more enhanced by neonatal TCDD treatment than those in control mice. These findings were consistent with the reports that TCDD enhances proliferation and cytokine production of mitogen- or Ag-stimulated T cells or T cell clones (1, 8). Because there were alterations in the percentage and number of DN cells in TCDD-treated mice, we analyzed this population using CD44 and CD25 markers. After TCDD treatment in this set, there was a decrease in the percentage of $CD44^+CD25^-$ cells (DN1) and $CD44^-CD25^-$ cells (DN4), and a relative increase in the percentage of $CD44^+CD25^+$ cells (DN2) and $CD44^-CD25^+$ cells (DN3). Analysis of the actual numbers of cells in each population compared with controls suggested that thymic maturation or negative selection at DN2 or DN3 might be affected by neonatal exposure to the low-dose TCDD. These results suggest that TCDD is interfering with the development and/or the proliferation of DN cells. Furthermore, the early stage of DN and the late stage into CD4SP or CD8SP in the thymic differentiation were disturbed by low-dose TCDD treatment, indicating that the immunotoxicity of TCDD on neonatal thymus might lead to the development of T cell-dependent autoimmunity. The inflammatory lesions were observed in the organs other than salivary gland including kidney, lung, and liver in TCDD-treated mice. Although the inflammatory lesions in liver, lung, and kidney from female mice treated with 10 ng of TCDD at 2 mo of age were observed, the severity of extraglandular lesions was lower than that of salivary gland, and the onset was later compared with that in salivary gland. Most of the extraglandular lesions of both female and male mice were developed with aging. We have previously demonstrated that the extraglandular lesion such as autoimmune arthritis in 3d-Tx NFS/*sld* mice was observed with aging (45, 46). Therefore, it is possible that TCDD may enhance any age-related reaction in the organs to induce autoimmunity.

In this study, there were no changes in the B cell number and proliferation in spleen from low-dose TCDD-treated mice, although the suppressive effect of the T cell-dependent Ab response to sheep RBC was reported in C57BL/6 mice injected with TCDD (47). In addition, TCDD selectively inhibited terminal B cell differentiation into plasma cells in response to trinitrophenol-LPS without altering early events in B cell activation or proliferation (48). By contrast, in our study significantly increased autoantibody productions such as anti-SSA/La, anti-SSB/Ro, and anti-α-fodrin were observed by neonatal exposure to low-dose TCDD. Although it is still unclear whether the direct or indirect effect of TCDD on B cells influences autoantibody production, this new finding may be a key to understand the association of TCDD immunotoxicity with the development of autoimmunity.

AhR is a cytoplasmic receptor protein and has been described as a ligand-activated transcription factor that mediates induction of xenobiotic metabolizing enzymes (27, 28, 49). Upon ligand binding, the AhR translocates into the nucleus and dimerizes with ARNT. The AhR/ARNT complex binds to specific gene promoter elements (50). In this study, significantly increased expressions of AhR mRNA and protein in neonatal thymus were observed compared with those in adult thymus. This suggests that neonatal exposure to low-dose TCDD may effect thymic differentiation and/or maturation through AhR by disrupting the T cell tolerance more intensively than those in adult thymus. If negative or positive selection in the neonatal thymus is disrupted by low-dose TCDD exposure, autoreactive T cells may be released to the periphery and expand in response to any autoantigen leading to induce autoimmunity. Increased expression of AhR mRNA and the disrupted thymic differentiation in the neonatal thymus by low-dose TCDD exposure may support this hypothesis.

CYP1A1 is known to have pivotal roles in cell growth and apoptosis (51, 52). In the present study, CYP1A1 mRNA of neonatal thymocytes was readily up-regulated by TCDD, whereas the expression of adult thymocytes was constant in the response to TCDD. Neonatal exposure to low-dose TCDD may influence proliferation, differentiation, or apoptosis of thymocytes through CYP1A1 at early stages, such as DN. Namely, it is possible that negative selection leading cell apoptosis at DN3 might be disturbed by neonatal exposure to TCDD. As a result, autoreactive T cells leaking from thymic selection might survive and proliferate in response to any autoantigen in the periphery, leading to the induction of autoimmune lesions. The activation of AhR by TCDD results in an increased binding activity to NF-κB subunit RelB of AhR itself to form AhR/RelB complex, which was associated with an increased mRNA level of multiple inflammatory genes (53). Overexpression of AhR and RelB led to an increased level of CCL1 and IRF-3 in control as well as TCDD-stimulated cells supporting the role of RelB and AhR for the transcriptional regulation of these genes (54). In the present study, TCDD enhanced TCR-mediated classical NF-κB activation of neonatal thymocytes from NFS/*sld* mice more than adult thymocytes. In addition, some NF-κB-target genes such as Bcl-x_L and TNF-α in thymus were up-regulated by in vivo TCDD injection. Our data demonstrate that

TCDD/AhR signal may influence the differentiation or development of T cells in the neonatal thymus associated with autoimmunity. However, the precise mechanism of how the NF-κB activation, including classical and nonclassical pathway, interacts with TCDD/AhR signal is still unclear.

It has been well known that autoimmune lesions of multiple organs such as lacrimal glands, salivary glands, pancreas, and liver are observed in AIRE gene-deficient mice (39). AIRE was reported to play a pivotal role in the expression of tissue-specific autoantigens such as salivary protein-1, GAD67, insulin, or other self-proteins in the TECs that express the MHC class II on the cell surface and function as APCs to immature T cells for the immunological selection of central tolerance in the thymus (55). In this study, mRNA expressions of AIRE and tissue-specific autoantigens such as salivary protein-1 and GAD67 in the thymus were reduced by the in vivo neonatal exposure to low-dose TCDD in NFS/*sld* mice. The finding indicated that TCDD might influence the selection of autoreactive T cells in the thymus through AIRE. There may be any complex molecular mechanisms related to the avidity of TCR, haplotype of MHC class II, Ag-specificity, T cell apoptosis, interaction with TEC, or TCDD signal.

The AhR has been shown to mediate various immunotoxic responses induced by environmental pollutants like TCDD (56). Although our results show that activation of the AhR by TCDD effects T cell development, the receptor does not seem to play a key role in the establishment of a normal T cell compartment. The AhR has been shown to play important roles in regulating the expression of several cytokines. For example, exposure of rats to TCDD led to up-regulation of IL-1β and TNF-α in the liver (57, 58). Interestingly, although TCDD suppressed the production of IFN-γ by mediastinal lymph node cells, there was a 10-fold increase in the IFN-γ level in the lungs of TCDD-treated mice (59). Autoimmune disease is caused by heterogeneous etiology, involving interplay between predisposing genes and triggering environmental factors. Although a lot of studies have demonstrated the immunotoxicity of TCDD, this study is the first to induce autoimmunity by neonatal low-dose TCDD treatment. Recently it has been reported that AhR links T_H17 cell-mediated experimental autoimmune encephalomyelitis to environmental toxins through altering the differentiation of Treg cells (60, 61). The low-dose TCDD exposure in our model had little influence on the number of Treg cells in spleen and the function of T_H17 cells, such as IL-17 production from T cells. The action of TCDD via AhR may influence peripheral tolerance related to autoimmunity besides central tolerance in thymus.

Taken together, our new findings may explain the risk for autoimmunity caused by the late effect of early exposure to environmental pollution, including TCDD. And as shown here, our model would help to understand the multifactorial nature of autoimmune disease.

Acknowledgments

We thank Ai Nagaoka, Noriko Kino, Risa Okada, Ritsuko Oura, and Satoko Yoshida for technical assistance.

Disclosures

The authors have no financial conflict of interest.

References

1. Kerkvliet, N. I. 2001. Recent advances in understanding the mechanisms of TCDD immunotoxicity. *Int. Immunopharmacol.* 2: 277–291.
2. Wormley, D. D., A. Ramesh, and D. B. Hood. 2004. Environmental contaminant-mixture effects on CNS development, plasticity, and behavior. *Toxicol. Appl. Pharmacol.* 197: 49–65.
3. Schecter, A., L. Birnbaum, J. J. Ryan, and J. D. Constable. 2006. Dioxins: an overview. *Environ. Res.* 101: 419–428.
4. Laiosa, M. D., A. Wyman, F. G. Murante, N. C. Fiore, J. E. Staples, T. A. Gasiewicz, and A. E. Silverstone. 2003. Cell proliferation arrest within intrathymic lymphocyte progenitor cells causes thymic atrophy mediated by the aryl hydrocarbon receptor. *J. Immunol.* 171: 4582–4591.
5. Gehrs, B. C., and R. J. Smialowicz. 1999. Persistent suppression of delayed-type hypersensitivity in adult F344 rats after perinatal exposure to 2,3,7,8-tetrachlorodibenzo-p-dioxin. *Toxicology* 134: 79–88.
6. Walker, D. B., W. C. Williams, C. B. Copeland, and R. J. Smialowicz. 2004. Persistent suppression of contact hypersensitivity, and altered T-cell parameters in F344 rats exposed perinatally to 2,3,7,8-tetrachlorodibenzo-*p*-dioxin (TCDD). *Toxicology* 197: 57–66.
7. Prell, R. A., E. Dearstyne, L. G. Steppan, A. T. Vella, and N. I. Kerkvliet. 2000. CTL hyporesponsiveness induced by 2,3,7,8-tetrachlorodibenzo-*p*-dioxin: role of cytokines and apoptosis. *Toxicol. Appl. Pharmacol.* 166: 214–221.
8. Prell, R. A., J. A. Oughton, and N. I. Kerkvliet. 1995. Effect of 2,3,7,8-tetrachlorodibenzo-*p*-dioxin on anti-CD3-induced changes in T-cell subsets and cytokine production. *Int. J. Immunopharmacol.* 17: 951–961.
9. Shepherd, D. M., E. A. Dearstyne, and N. I. Kerkvliet. 2000. The effects of TCDD on the activation of ovalbumin (OVA)-specific DO11.10 transgenic CD4(+) T cells in adoptively transferred mice. *Toxicol. Sci.* 56: 340–350.
10. Morris, D. L., J. G. Karras, and M. P. Holsapple. 1993. Direct effects of 2,3,7,8-tetrachlorodibenzo-p-dioxin (TCDD) on responses to lipopolysaccharide (LPS) by isolated murine B-cells. *Immunopharmacology* 26: 105–112.
11. Karras, J. G., and M. P. Holsapple. 1994. Inhibition of calcium-dependent B cell activation by 2,3,7,8-tetrachlorodibenzo-*p*-dioxin. *Toxicol. Appl. Pharmacol.* 125: 264–270.
12. Dooley, R. K., D. L. Morris, and M. P. Holsapple. 1990. Elucidation of cellular targets responsible for tetrachlorodibenzo-p-dioxin (TCDD)-induced suppression of antibody responses. II. The role of the T-lymphocyte. *Immunopharmacology* 19: 47–58.
13. Gotter, J., and B. Kyewski. 2004. Regulating self-tolerance by deregulating gene expression. *Curr. Opin. Immunol.* 16: 741–745.
14. Anderton, S., C. Burkhart, B. Metzler, and D. Wraith. 1999. Mechanisms of central and peripheral T-cell tolerance: lessons from experimental models of multiple sclerosis. *Immunol. Rev.* 169: 123–127.
15. Miller, J. F., and R. A. Flavell. 1994. T-cell tolerance and autoimmunity in transgenic models of central and peripheral tolerance. *Curr. Opin. Immunol.* 6: 892–899.
16. Kruize, A. A., R. J. Sweenk, and L. Kater. 1995. Diagnostic criteria and immunopathogenesis of Sjögren's syndrome: implications for therapy. *Immunol. Today* 16: 557–559.
17. Fox, R. I., M. Stern, and P. Michelson. 2000. Update in Sjögren syndrome. *Curr. Opin. Rheumatol.* 12: 391–398.
18. Fox, R. I. 2005. Sjögren's syndrome. *Lancet* 366: 321–331.
19. Haneji, N., H. Hamano, K. Yanagi, and Y. Hayashi. 1994. A new animal model for primary Sjögren's syndrome in NFS/*sld* mutant mice. *J. Immunol.* 153: 2769–2777.
20. Haneji, N., T. Nakamura, K. Takio, K. Yanagi, H. Higashiyama, I. Saito, S. Noji, H. Sugino, and Y. Hayashi. 1997. Identification of α-fodrin as a candidate autoantigen in primary Sjögren's syndrome. *Science* 275: 604–607.
21. Saegusa, K., N. Ishimaru, K. Yanagi, K. Mishima, R. Arakaki, T. Suda, I. Saito, and Y. Hayashi. 2002. Prevention and induction of autoimmune exocrinopathy is dependent on pathogenic autoantigen cleavage in murine Sjögren's syndrome. *J. Immunol.* 169: 1050–1057.
22. Suri-Payer, E., K. Wei, and K. Tung. 2001. The day-3 thymectomy model for induction of multiple organ-specific autoimmune diseases. *Curr. Protoc. Immunol.* 15: 15–16.
23. Kojima, A., Y. Tanaka-Kojima, T. Sakakura, and Y. Nishizuka. 1976. Spontaneous development of autoimmune thyroiditis in neonatally thymectomized mice. *Lab. Invest.* 34: 550–557.
24. Teague, P. O., E. J. Yunis, G. Rodey, A. J. Fish, O. Stutman, and R. A. Good. 1970. Autoimmune phenomena and renal disease in mice: role of thymectomy, aging, and involution of immunologic capacity. *Lab. Invest.* 22: 121–130.
25. Tung, K. S., S. Smith, P. Matzner, K. Kasai, J. Oliver, F. Feuchter, and R. E. Anderson. 1987. Murine autoimmune oophoritis, epididymoorchitis, and gastritis induced by day 3 thymectomy. *Am. J. Pathol.* 126: 303–314.
26. Safe, S. 2001. Molecular biology of the Ah receptor and its role in carcinogenesis. *Toxicol. Lett.* 120: 1–7.
27. Denison, M. S., and S. Heath-Pagliuso. 1998. The Ah receptor: a regulator of the biochemical and toxicological actions of structurally diverse chemicals. *Bull. Environ. Contam. Toxicol.* 61: 557–568.
28. Marlowe, J. L., and A. Puga. 2005. Aryl hydrocarbon receptor, cell cycle regulation, toxicity, and tumorigenesis. *J. Cell. Biochem.* 96: 1174–1184.
29. Nohara, K., H. Fujimaki, S. Tsukumo, K. Inouye, H. Sone, and C. Tohyama. 2002. Effects of 2,3,7,8-tetrachlorodibenzo-*p*-dioxin (TCDD) on T cell-derived cytokine production in ovalbumin (OVA)-immunized C57Bl/6 mice. *Toxicology* 172: 49–58.
30. Neff-LaFord, H. D., B. A. Vorderstrasse, and B. P. Lawrence. 2003. Fewer CTL, not enhanced NK cells, are sufficient for viral clearance from the lungs of immunocompromised mice. *Cell. Immunol.* 226: 54–64.
31. Tomita, S., H. B. Jiang, T. Ueno, S. Takagi, K. Tohi, S. Mackawa, A. Miyatake, A. Furukawa, F. J. Gonzalez, J. Takeda, T. Ichikawa, and Y. Takahama. 2003. T cell-specific disruption of arylhydrocarbon receptor nuclear translocator (Arnt) gene causes resistance to 2,3,7,8-tetrachlorodibenzo-*p*-dioxin-induced thymic involution. *J. Immunol.* 171: 4113–4120.
32. Camacho, I. A., N. Singh, V. L. Hegde, M. Nagarkatti, and P. S. Nagarkatti. 2005. Treatment of mice with 2,3,7,8-tetrachlorodibenzo-*p*-dioxin leads to aryl